Elsevier Editorial System(tm) for
Microporous & Mesoporous Materials
Manuscript Draft

Manuscript Number: MICMAT-D-16-00955R1

Title: Acidity and basicity of zeolites: a fundamental approach

Article Type: SI: Zeolites & sustainability

Keywords: acidity; basicity; zeolites; adsorption; catalysis

Corresponding Author: Professor Guido BUSCA, Full Professor

Corresponding Author's Institution: University of Genoa

First Author: Guido BUSCA, Full Professor

Order of Authors: Guido BUSCA, Full Professor

Abstract: The main data concerning acidity and basicity characterization of protonic and cationic zeolites are described and discussed. In particular, experimental data concerning IR studies of the adsorption of pyridine, CO and CO2 on Na-zeolites (Na-X, Na-A, Na-MOR) and on protonic zeolites (with emphasis on H-Y and USY) are described and discussed. The nature of the Lewis acid and basic sites as well as of the Brønsted acid sites is discussed with a fundamental chemical approach.

Ms. Ref. No.: MICMAT-D-16-00955

Title: Acidity and basicity of zeolites: a fundamental approach

Microporous & Mesoporous Materials

Reviewer #1:

The manuscript reports an overview of the study of both acid and basic properties of zeolites monitored by IR spectroscopy of adsorbed probe molecules, in particular pyridine, CO and CO2. Particular emphasis is given to the discussion of Lewis acid and basic sites contained in zeolites. Although the treated argument is largely studied in the literature, the manuscript represents an organized review work, in which data are discussed taking into account the chemical properties of studied materials.

In my opinion, the work merits publication after minor revisions as indicated below.

1) Details on the origin and chemical composition of zeolites that are studied in the paper as well as on the experimental parameters used to collect FTIR data should be added.

A "Materials and experimental methods" section has been added in the revised text, where these data are provided.

2) It would be probably better to introduce the paragraphs 2.3 and 2.4, related to the description of the structure of FAU and LTA zeolites, before of the sections related to the study of acido-basicity of the same materials.

The original chapters 2.3 and 2.4 have been displaced and are now chapters 2.1 and 2.2 in the revised manuscript.

2) In Paragraph 2.1, results related to Pyridine adsorption on NaX zeolite are reported (Fig.1). Unfortunately, as also stated from the author, the adsorbed Pyridine was contaminated by water, as it is also visible from the IR analysis (band at 1650 from Fig. 1). It is probably better to repeat the experiment using a well-dried probe molecule.

The water adsorption affinity of NaX is so strong that is very difficult to avoid small amounts of water to be present on the surface during contact with adsorbates. On the other hand, the experiments done trying to have almost no water do not give rise to different spectra of pyridine adsorbed species. As we have shown also on other surfaces, in fact, pyridine is a stronger base than water and displaces it from adsorbing sites. This is an interesting result. Thus, we would like to live the data as such.

Please add the indication of the band at 1441 cm-1 in Fig. 1.

Done

3) CO molecule was also used to study the same NaX zeolite (Fig. 2). The author should explain why evacuation is performed by increasing the temperature and not at constant T, as normally did in the literature. Evacuation at the same temperature at which CO adsorption is performed could be more interesting to have indication on the stability of the different surface sites interacting with CO.

As explained in the new experimental section, our cell can work down to 130 K, i.e. real sample temperature measured by a thermocouple, when the external reservoir of the cell is full of liquid nitrogen. The temperature depends on the level of liquid nitrogen in the reservoir. Indeed we generally warm very slowly, leveing nitrogen free evaporation. Actually the temperature change is much slower than the recording time (one minute scanning) thus the temperature is nearly constant during the measurement.

The presence of residual Bronsted acid sites (that was pointed out by Py adsorption) is also visible on the high frequency of the IR spectra obtained upon CO adsorption?

Yes, indeed. We can see the free OH band…

Lettering should be added to Fig. 2 to have a better definition of conditions (i.e. variation of temperature and/or pressure) used to collect the different IR spectra.

Done

4) The author should discuss the reasons why carbonate species formed upon CO2 adsorption in NaX, NaA and NaMOR zeolites are different.

Done

5) Graphical abstract should be revised to be more representative of the meaning of the manuscript.

The graphical abstract has been modified

Reviewer #2: This is a very useful and inclusive review paper summarizing all relevant information produced so far on structure and reactivity of zeolites. The questions which are still open, in spite of the massive research work, are very clearly pointed out.

Very few misprints have been found, such as:

Pag.1- bottom: a word is missing after "still a ..." **corrected**

Pag.14 - last line: Is Fig.11 properly quoted? **yes**

Pag. 16 - lines 2-3: a verb is missing. **corrected**

Fig. 1 - The peak around 1440 might be labelled as the others are. **done**

Fig. at pag 41 - it is mislabelled a Fig.9 instead of Fig. 14 **corrected**

Reviewer #3: The manuscript "Acidity and basicity of zeolites: a fundamental approach" by Guido Busca is a comprehensive review of the most significant data and features concerning the spectroscopic (mainly IR) characterization of the acidity and basicity of zeolites.

The paper is well organized and clearly discussed. Despite the lack of novel insights, as a whole the paper is a useful and interesting review for researchers dealing with the spectroscopic characterization of acid and basic zeolites.

Some concern arises from paragraphs 2.3 and 2.4, where basic knowledge of zeolites chemistry and structures of well-known zeolites are described in details. These paragraphs appear pleaonastic and should be modified or even eliminated.

According to the comment of reviewer #1 these paragraphs were displaced. We agree that, for specialists in zeolites, the description of these structures is unnecessary. However, for people not deeply involved in the zeolites field we believe that it is useful or even necessary, to explain how the different zeolite structures may imply a different behavior, even in the absence of the well-known molecular sieving effect. Thus, we would prefer to retain this description.

Minor comments are the following:

- Graphical abstract: In the scheme related to cationic zeolites, it seems that a negative charge is formalized on two oxygen atoms bonded to Al. Actually only one negative charge is introduced in the framework by the substitution of a silicon atom with an aluminum. Indeed in the same scheme only one sodium ions appears close to the aluminum site.

Actually if we consider a zeolite with the formula NaSiAlO4, this may be considered as a Na,Al orthosilicate. In this case all oxygen atoms of the orthosilicate anion [SiO4]4- are negatively charged. The charge of Al3+ must be also considered.

Some concern also arises from the coordinative bonds of two oxygens with one aluminum in the same scheme. In the scheme related to the protonic zeolites, the coordinative bond should involve only the silanol.

This is questionable, in our opinion. In fact all four Al-O bonds in a tetrahedral group are essentially ionic, thus they are coordination bonds from the anionic oxygens to the Al3+ cation.

- Page 13, line 9. The author reports that "the trend among different studies is for increased chemical shift corresponding to an increase in the intrinsic acidic strength (proton affinity)". Proton affinity is not a measure of the intrinsic acidic strength of a BrÃ¶nsted acidic site. Does the author mean "deprotonation energy"? If this is not the case, what does the author mean?

Indeed we took exactly the statement published in the reference. On the other hand, the reviewer is right. Probably the authors of the cited reference refer to something like “the inverse” of the proton affinity. In any case we cancelled the commas and its content (proton affinity) in the revised text.

***Highlights (for review)**

- Spectroscopic features of cationic and protonic zeolites are discussed critically
- Orthosilicate species in high Al zeolites have relevant basicity
- Cationic zeolites have strong ionicity and moderate Lewis acido-basicity
- Stabilization of anionic charge by Si-O-Si bridges is crucial for H-zeolites acidity
- Stabilization of protonated species by cavities is also key for H-zeolites acidity

*Graphical Abstract

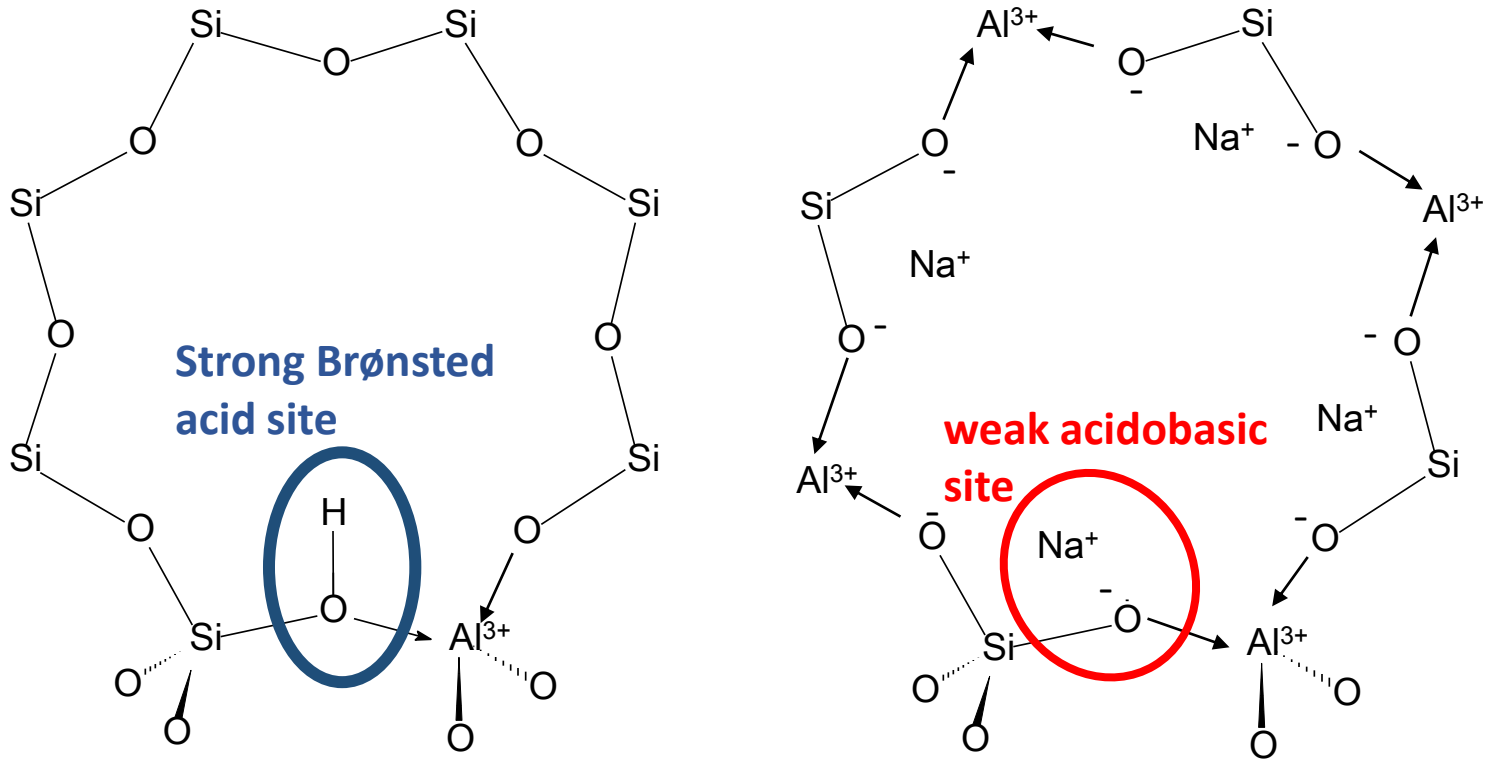

Acidity and basicity of zeolites: a fundamental approach *[1]

Guido Busca
Dipartimento di Ingegneria Civile, Chimica e Ambientale (DICCA), Università degli Studi di Genova, P. J.F. Kennedy, 1 16129 Genova, Italy

Keywords: acidity; basicity; zeolites; adsorption; catalysis.

Abstract: The main data concerning acidity and basicity characterization of protonic and cationic zeolites are described and discussed. In particular, experimental data concerning IR studies of the adsorption of pyridine, CO and CO_2 on Na-zeolites (Na-X, Na-A, Na-MOR) and on protonic zeolites (with emphasis on H-Y and USY) are described and discussed. The nature of the Lewis acid and basic sites as well as of the Brønsted acid sites is discussed with a fundamental chemical approach.

1. Introduction.

Protonic zeolites represent today the most prominent class of environmentally friendly solid acid catalysts, largely used in industry for catalytic cracking, alkylations, skeletal isomerizations, etc. [1,2,3,4,5]. Some transition metal-containing zeolites find application as redox catalysts, such as for catalytic reduction of NOx with ammonia [6,7] and for the abatement of N_2O by decomposition [7,8] and reduction with methane [8]. Alkali and alkali earth cationic zeolites are largely used as industrial adsorbents for gas purification [9] including CO_2 capture [10], to produce membranes for gas separations [11], and as ion exchangers for water softening [12]. The possible application of cationic zeolites as “basic catalysts” is mentioned [13,14] but actual industrial applications seem to be still absent [15,16]. The discovery and application of zeolites has been strictly linked with the development of refinery and petrochemistry, but these materials will have a key role also in the re-starting era of chemistry based on biomass conversion [17].

In most of their applications, acidity and basicity of zeolites are key properties. In spite of this very relevant practical role, still a lot of questions are open concerning the behavior of zeolites, in particular as acid and basic materials.

[1] Based on the lecture given at the IZC18 Preconference School in Campinas (Brazil), june 2016.

In this paper, the acido-basic properties of zeolites are reconsidered, based on spectroscopic measurements and on the known catalytic and adsorption behavior, with a fundamental chemical approach.

2. Materials and experimental methods.

Data on the materials used in the experiments reported in the paper are reported in Table 1. Fourier Transform InfraRed (FTIR) spectra were recorded using Nicolet 380 FT-IR spectrometers. Adsorption/desorption studies were performed using the pure powders pressed into thin wafers and activated in the IR cell, connected with a conventional outgassing/gas-manipulation apparatus. Activation was performed by heating under vacuum (10^{-3}-10^{-5} Torr) at 773 K. The activated samples were contacted with vapour / gases (water, pyridine and CO_2) at room temperature (r.t.) for 15 min; later, the IR spectra of the surface species were collected in continuous evacuation at room and increasing temperatures. CO adsorption (30 Torr) was performed at 130 K (real sample temperature measured by a thermocouple, when the external reservoir of the cell is full of liquid nitrogen) by the introduction of gaseous CO inside the liquid nitrogen cooled low temperature infrared cell containing the previously activated wafers. IR spectra were collected under evacuation upon warming at increasing temperatures between 130 and 273 K, as the result of the progressive decrease of the level of liquid nitrogen in the cell reservoir..

3. Acido-basicity of cationic zeolites: the case of on Na-zeolites.

3.1 Structural chemistry of cationic zeolites.

Zeolite's structure can be viewed as derived from a microporous silica polymorph, such as a "silicalite". The substitution of aluminum for silicon in a silica covalent framework leads to a charge un-balance which must be compensated by "extra-framework" cations, mostly alkaline. This occurs also for non-zeolitic systems such as in the cases of the so-called "stuffed silicas". Stuffed silicas are alkali aluminosilicates with structures strictly related to the crystalline forms of silica, but with Al ions substituting for Si in the framework and alkali cations in the interstices to counterbalance the resulting charge defect. This is the case, for example, of β-eucriptite ($LiAlSiO_4$, a stuffed β-quartz), where Li^+ ions enter "extra-framework" tetrahedral interstices of the quartz framework, or nepheline ($NaAlSiO_4$, a stuffed tridymite) where the larger Na^+ ions enter extra-framework octahedral interstices of

the tridymite structure. Interestingly, these solids have ion-exchange capacity [18,19]. A similar mechanism also occurs in the amorphous networks of silicoaluminate glasses [20].
In the case of natural and “cationic” zeolites, the balancing cations (usually alkali or alkali earth ions) are located in relatively large cavities formed by the $[Si_{1-x}Al_xO_2]^{x-}$ negatively charged framework, where $x \leq 0.5$, which means that the Si/Al atomic ratio never is lower than 1 (Lowensteins' rule [21]). The cations are exchangeable, thus zeolites may also act as cationic exchangers. The exchange can be performed with ammonium ions which can be later decomposed into gaseous ammonia and a proton. This allows to produce protonic zeolites, which are very strong solid Brønsted acids. Today, protonic zeolites are mostly synthesized directly, by using templating agents. In this case the protons may be residual from the combustion or decompostion of the templating agents.

3.2 Faujaste Na-X and zeolite Na-LTA: zeolitic sodium,aluminum orthosilicates.

Sodium zeolites are denoted by the formula $Na_xSi_{1-x}Al_xO_2$, where $x \leq 0.5$. In the case of faujaste Na-LSX (Low Silica X) and zeolite Na-LTA, $x \sim 0.5$, i.e. Si/Al atomic ratio is ~ 1, thus the formula is $NaSiAlO_4$. This makes these zeolites polymorphic forms of nepheline, a stuffed derivative of tridymite, and carnegierite, a stuffed derivative of cristobalite, all characterized by the formula $NaSiAlO_4$. As also in the case of nepheline and carniegite, Si and Al essentially regularly alternate in the tetrahedral-based framework, thus producing sodium, aluminum orthosilicates: orthosilicate anions are formed, whose oxygen atoms are ionically bonded to one tetrahedrally coordinated Al^{3+} cation each and to at least one Na^+ ion each.
The ideal faujasite structure (Fig. 1) is formed by wide supercages (13 Å diameter) accessed through 12-member silicate rings (12MR) with 7.4 Å diameter, much smaller sodalite cages accessed through 6-member silicate rings (6MR) and hexagonal prisms connecting the sodalite cages. The stoichiometry of the unit cell of a Na-LSX zeolite is $Na_{96}[Al_{96}Si_{96}O_{384}]$, containing 8 sodalite cages, 8 supercages and 16 hexagonal prisms. Four crystallographically different oxygen atoms exist in the structure (Fig. 1), two of which (1 and 4) point into the supercage, one (2) into the sodalite cage, and the fourth (3) into the hexagonal prism. Several possible extraframework cationic positions may be occupied [22,23]. In dry faujasites, Na^+ cations sit on different sites called site I (with the alternative of site I’), site II, and site III (with the alternatives of site III’a and III’b [24]). Site I is in the center of the hexagonal prism (16 per unit cell) while the alternative sites I’ are just over of the 6MR in the sodalite cage (32 per unit cell). Site II (32 per unit cell) is just above the

center of the 6MR separating supercages and sodalite cages. Site III (48 per unit cell) is just above the 4MR separating separating supercages and sodalite cages, but has alternatives in sites III', III'a and III'b, in near positions off center the 4MR [24].

A theoretical perfect Na-LSX zeolite, with Si/Al ratio = 1, has full occupation of sites I and II, and essentially half occupation of sites III, with no occupation of sites I', III'a and III'b. In the case of Na-X zeolite, with Si/Al ratio 1.2-2, occupancy of sites I is < 1, with some occupancy of sites I', occupation of site II is still essentially full, while occupancy of sites III is low, the alternative sites III'a and III'b being mainly occupied. Due to the small size of the windows, most authors (except few [25]) suppose that sodalite cages and hexagonal prisms, where sites I and I' are located, are inaccessible to polyatomic molecules. Thus, all the adsorption and catalysis chemistry of faujasites would occur in the supercages. These large cavities contain (in the real Na-X structure) in average a little less than 10 Na^+ ions, 4 of which are located at site II and a little less than 6 located in sites III'a and III'b. Na^+ ions in sites II are bound to three O(2) oxygen atoms of the 6MR, those in site III'a are only coordinated to one O (4), but interacts also with two O (1) atoms, those in site III'b interact only with two O (4) and one O (3) oxygen atom. Thus, these Na^+ ions have very low overall coordination with quite weak coordination bonds, and may also be influenced by their mutual electrostatic repulsion.

Zeolites denoted with the LTA code (Linde Type A, Fig. 2) are small pore zeolites characterized by a cubic structure. The sodium form is another $NaSiAlO_4$ polymorph. Also in this case, the stoichiometry of the "perfect" unit cell is $Na_{96}[Al_{96}Si_{96}O_{384}]$, containing 8 α cages (or supercages), and 8 β cages (sodalite cages). The sodium ions occupy three main sites [26], referred to as site I, II and III, all located nearly at the external surface of the supercages. Sites I, fully occupied, are located at the centers of the 6MRs separating sodalite cages from supercages, with a very small displacement away from the plane of the ring toward the sodalite-cage. Sites II are located at sites associated with the 8MRs separating supercages each other, in the plane of the ring but offset from the ring center, interacting with three oxygen atoms in the ring. Sites II are nearly half occupied, with nearly one Na atom per 8MR. The occupancy of site III, located above the center of the 4MRs, is 5-8%, random. In average, the supercages, that have a diameter of near 11.5 Å, contain 12 Na^+ atoms. Thus the supercages of zeolite Na-LTA are smaller but contain more sodium ions than the supercages of zeolite Na-X.

3.3. Structure of Na-Mordenite.

Mordenite, in its most stable and common forms, both natural and synthetic, are characterized by a relatively high Si to Al atomic ratio, most commonly > 4-6. Thus, Si-O-Si bridges exist, corresponding to polysilicate species. The orthorombic mordenite structure (Fig. 3 [27]) is characterized by nearly straight “main” channels running along the [001] crystallographic direction, which are accessible through twelve-membered (elliptical) silicon-oxygen rings having 6.5 Å x 7.0 Å diameters. Additionally, 8-ring “side pockets” exist in the [010] direction having 3.4 Å x 4.8 Å diameter, which however do not allow flow of molecules being in fact interrupted by narrow-necked obstructions. The side pockets connect the twelve ring main channel to a distorted eight-ring compressed channel also running parallel to the [001] direction, but having a elliptical compressed opening 5.7 Å x 2.6 Å wide. The location of Na^+ in Na-MOR samples has been the object of several studies [28,29,30]. Assuming the idealized composition for dehydrated MOR $Na_8Si_{40}Al_8O_{96}$ (Si/Al = 5) it seems quite established that half of Na^+ ions are located just in the middle of the small compressed channels in the site called (I) or A. Location (I) or A is also fully occupied for MOR samples with Si/Al = 11. It is usually supposed that only monoatomic species can enter the smaller channels of NaMOR, thus being supposed to be not available for CO. The other half Na^+ ions are distributed between site IV, also called D, near the opening of the side pocket in the main channel, and in position VI, also called E, which is well exposed in the main channel. The theoretical occupation degree of each site is 4,3,1 for A,D,E [28]. The cations in position IV (near the center of a 8MR) appear to be more shielded by oxygens than those at position VI (off center of a 6MR).

3.4 Characterization of the acidity of sodium zeolites using FTIR of adsorbed basic probe molecules.

The characterization of the surface acid and basic properties of solids is mostly accomplished using adsorption of molecular probes. Among the many basic probe molecules proposed to characterize the surface acidity of catalytic materials, including zeolites [31], pyridine and CO are the most largely applied [32,33]. They are also in some way complementary probes, because pyridine is a moderately strong base with poor volatility, while CO is a very weak base with high volatility. CO adsorption on acidic sites occurs by interaction of its lone pair at C atom. It must be studied at low temperature (77-150 K) to detect its very weak interaction with Lewis sites (coordination or polarization) and Brønsted sites (H-bonding). Instead, pyridine adsorption can be studied at r.t. or even

higher temperatures, due to the strength of the interactions produced: coordination on Lewis acid sites, H-bonding or protonation on Brønsted acid sites. Taking into account proton affinity (PA) data for measuring gas-phase basicity, CO (PA ~ 594 kJ/mol) is weaker as a base even than most saturated hydrocarbons acting as σ-bases (e.g. PA of propane ~ 625 kJ/mol) as well as of the unsaturated hydrocarbons (olefins and aromatics) acting as π–bases (PA ÷ 680-810 kJ/mol). In contrast, pyridine (PA ~ 950 kJ/mol) is even a stronger base than most n-bases, including water molecule (PA ~ 700 kJ/mol) and water clusters (PA ~ 940 kJ/mol) [34]. This makes data arising from CO adsorption useful in relation to reactions performed in dry atmospheres with weak basic molecules such as hydrocarbons, and data arising from pyridine adsorption more useful in relation to reactions performed in wet atmospheres and/or with strong basic reactants.

The IR spectra of pyridine adsorbed on NaX are reported in Fig. 4. The main bands observed at high coverages at 1590, 1573, 1488 and 1441 cm^{-1} are due to the 8a, 8b, 19a and 19b modes of adsorbed molecular pyridine. The maxima of the sensitive 8a and 19b bands (1590 and 1441 cm^{-1}) are both slightly shifted up with respect to the liquid pyridine values of 1580 and 1438 cm^{-1} [35], showing interaction with a weak electron-withdrawing site.

By progressive outgassing, the 19b mode progressively decreases in intensity but its maximum progressively shifts up to 1444 cm^{-1}. On the other hand, the 8a mode is clearly complex, showing two main maxima at 1590 and 1613 cm^{-1}. By outgassing, the former component decreases faster in intensity also shifting up to 1595 cm^{-1} while the latter decreases slower in intensity without a relevant shift, but disappears later leaving another weak residual band at definitely higher frequency (1622 cm^{-1}).

During the adsorption and desorption experiments a broad band also appears at 1650 cm^{-1}, that is associated to an absorption centered near 3450 cm^{-1}, in the OH stretching region. These features decrease progressively in intensity down to disappear by outgassing at 373 K (i.e. well before desorption of pyridine). They can be attributed to adsorbed water coming with pyridine vapour. We have confirmed that pyridine, being a stronger base than water, displaces water from its adsorption sites. Thus, the spectra of adsorbed pyridine are not modified in the presence of small amounts of water.

The largely predominant species formed by pyridine adsorption on NaX, well evident also when some water is present, is certainly molecular pyridine adsorbed on weakly Lewis acidic Na^+ cations, responsible for 8a and 19b bands at 1590-1595 cm^{-1} and 1441-1444 cm^{-1}, respectively, in agreement with previous studies [36,37]. The shifts of the bands

upon outgassing are indicative of some heterogeneity of the Na^+ sites in NaX. Another molecular pyridine species, associated to definitely weaker bands but bonded to stronger Lewis acid sites, is responsible for the 8a band at 1613 cm^{-1}; these sites may be very highly exposed Na^+ ions, or Al^{3+} ions. A third molecular species, responsible for the 8a mode at 1622 cm^{-1}, which is certainly associated to pyridine adsorbed on some alumina or silica-alumina debris [31]. A fourth species is responsible for the very weak 19a mode of pyridinium ion at 1546 cm^{-1}, showing that few Brønsted sites are present or are formed during pyridine (and some water) adsorption and desorption, present either on structural defects or on binding matter.

Fig. 5 shows the IR bands of CO adsorbed at low temperature on NaX zeolite. At temperatures lower than 163 K, mainly one asymmetric and very intense band (maximum out of scale) is observed in the CO stretching range. With outgassing at increasing temperatures, the intensity of this band diminishes, the main maximum being found at 2165 cm^{-1} with a shoulder at 2176 cm^{-1}. Additionally, other two bands with very weak intensity, located at 2138 cm^{-1} and 2115 cm^{-1} are present. By progressively increasing temperature upon outgassing, the intensities of the main band and of its shoulder (that at low surface coverage shifts up to 2182 cm^{-1}) decrease in parallel, while the two lower frequency components disappear even earlier. The band at 2139 cm^{-1}, located near the frequency of liquid CO, disappears completely quite fast in vacuum and therefore can be attributed with confidence to pseudo-liquid (physisorbed) CO inside the zeolite pores. The main bands at 2165 cm^{-1} and 2176 cm^{-1} are certainly due to CO interacting, through the C atom, with two different Na^+ ions [38]. Accordingly, their CO stretching frequency is shifted up with respect to the liquid phase value. In agreement with the structure of NaX, described above, the main band at 2164 cm^{-1} is assigned to CO C-bonded to SII site cations, and the shoulder at 2175 cm^{-1} is assigned to CO C-bonded to III'a and III'b site cations. The very weak band at 2115 cm^{-1}, located below the CO stretching of pure ^{12}CO, can be attributed to O-bonded CO species ($Na^+\cdots OC$) although C-bonded ^{13}CO and a component of sodium-dicarbonyl species may contribute to it [39].

The spectra of CO and pyridine adsorbed on NaX confirm the moderate Lewis acidity of the Na^+ cations in the faujasite supercage. The spectra of CO also provide evidence of the presence of at least two well different cationic sites. Very small amounts of stronger Lewis sites (likely Al^{3+}) and Brønsted sites, revealed by pyridine adsorption, are possibly associated to structural defects or binding matter present in the sample.

Due to the small cavity windows, pyridine cannot enter the cavities of Na-A zeolite. In contrast, CO can enter the supercages of this zeolite, while the entrance in the sodalite cavities is unallowed also for CO. The spectra of adsorbed CO (Fig. 6, left) show a main band at 2164 cm^{-1}, assigned to C-bonded CO species over Na^+ ions. The band is highly symmetrical without any relevant splitting. Additionally, different weak lower frequency components are observed, due to species whose stabilities to outgassing appears to be stronger. Also the band at 2146 cm^{-1} could be attributed to CO C-bonded on a single Na^+ ion, although its stability (stronger than that of the band at 2164 cm^{-1}, in contrast with the lower CO stretching frequency) can be explained by a further weak interaction, either with the O lone pair or/and with the π- type bonding electron pair. The band at 2112 cm^{-1} seems to be due to a highly stable species. According to its stretching frequency, lower than that of free CO, to justify its stability and its CO stretching frequency, this band must be attributed to CO interacting with more than one cation, likely through both the carbon and the oxygen atom. Also the band at 2128 cm^{-1}, should be due to species forming a different complex interaction.

In Fig. 6, right, the spectra of CO adsorbed on Na-MOR are also compared. On Na-MOR, the main CO stretching band shows components at 2177 and 2164 cm^{-1}, attributed to C-bonded CO species over two different Na^+ ions [40,41,42,43]. The cations in position IV (near the center of a 8MR) appear to be more shielded by oxygens than those at position VI (off center of a 6MR), and this allows us to assign the higher frequency component to CO C-bonded at position VI cations, the lower frequency one being assigned to CO C-bonded at position IV cations.

The component at 2138 cm^{-1} instead, which is the most stable upon outgassing and whose CO stretching frequency is lower, has been attributed by us to CO bonded to two cations with C and O atoms respectively [42,44].

The relative intensity of the low-frequency / strong interaction band with respect to that of the high-frequency band due to usual C-bonded carbonyls is much higher for Na-MOR than for Na-LTA, in spite of the higher Na (and Al) content of A type zeolite with respect to MOR. However, while the pore size of Na-LTA (~ 4 Å for the 8MR) is definitely smaller than that the main channels of Na-MOR (~ 6,5 Å), the size of the cavity (i.e. of the supercages) of Na-LTA (more than 10 Å) is far larger. So couples of sufficiently near Na ions may be more frequent in Na-MOR than in Na-LTA. On the other hand, the CO stretching frequency of the more intense band that can be assigned to multiple interaction

is in the case of Na-LTA at a definitely lower frequency (2112 cm^{-1}) than in the case of Na-MOR (2138 cm^{-1}) possibly due to a lower Na-Na distance.

The data reported here suggest that the medium Lewis acidity of Na sites is a most relevant property of Na-zeolites. We can note that the size and may be shape of the cavity (cages, channels), as well as the composition in terms of Na and Al content, may have a role in favouring, in particular, multiple interactions, providing more sites with more favourable positions.

3.5 Characterization of the basicity of sodium zeolites using FTIR of adsorbed CO_2.

A number of molecules have been proposed as probes for the surface basicity of oxide materials including zeolites. As discussed elsewhere [45], carbon dioxide is actually a good probe for the evaluation of medium-strong basicity, taking into account the nature of the species formed during adsorption as well as their thermal stability.

Adsorption of carbon dioxide on a dry 13X zeolite sample (Fig. 7) results in a quite complicated spectrum. Molecularly adsorbed carbon dioxide is observed, giving rise, at low coverage, to two components at 2345 and 2353 cm^{-1}, poorly resolved, due to the asymmetric OCO stretching (ν_3, 2349.3 cm^{-1} in the gas phase species) [46]. In the lower frequency region several bands are observed. The spectrum suggests the formation of carbonate-like species with the participation of framework oxygen atoms [47]. Upon outgassing, some of the low frequency bands increase in intensity, while bands of molecularly adsorbed CO_2 decrease strongly in intensity. The behaviour suggests that these bands can be grouped in several pairs. A quite strong couple of bands growing upon outgassing at 1488, 1432 cm^{-1} is assignable to monodentate carbonates. Bands observed at 1709, 1362 cm^{-1}, also growing upon outgassing, can traditionally be assigned to “organic-like” or “covalent” carbonates, but are most likely due to “strongly perturbed” bent CO_2 molecules [48]. The position of these bands is similar to that observed for bent CO_2^- metal complexes [49]. The shoulders at 1685, 1379 cm^{-1} could be due to similar species or to bicarbonate species, while the band at 1581 cm^{-1}, stable to outgassing, might be associate to another component in the 1450-1350 cm^{-1} range, and attributed to stable bidentate or chelating carbonate species. After outgassing at 473 K residual bands are still observed at 1653, 1487 and 1430 cm^{-1}, showing that on NaX relatively strong basic sites exist.

The spectrum observed on the 4A (Fig. 8), shows couples of bands at 1736, 1248 cm^{-1}, strong in contact with the gas, certainly due to a very labile species, likely “strongly perturbed” bent CO_2 molecules [48]. After outgassing several components in the 1700-

1500 cm^{-1} region (at 1693, 1665, 1640, 1593, 1569 cm^{-1}) likely correspond to components in the 1400-1250 cm^{-1} range (main features at 1383, 1359, 1340 cm^{-1}): these bands are attributed to bidentate or chelating carbonate species, while the band at 1457 cm^{-1} may be due to trigonal or monodentate carbonates. Adsorbed species are still found at least up to 390 K.

Bands due to carbonate-like species are also observed, together with adsorbed CO_2 molecules, after adsorption on Na-MOR (Fig. 9). In the figure the absorptions observed on Na-MOR are compared with those observed in the same conditions over H-MOR. In the latter case, essentially only linear CO_2 adsorbed species are observed (bands at 2360 and 1380 cm^{-1}, asymmetric and symmetric CO_2 stretching, respectively, the latter activated in IR due to the asymmetry generated by adsorption). This confirms that the "basic" sites where carbonate species form, are typical of cationic zeolites, while they do not exist on protonic zeolites, see below. The structure, and consequently the IR spectra and the thermal stability, of the carbonate species on different Na-zeolites are different, due to the different geometry and occupancy (in terms e.g. of number and location of Na ions) of the corresponding cavities. The stability of these species, however, is moderately weak: full desorption is usually observed in the range 400-500 K, showing that Na-zeolites are weaker, as bases (nucleophiles), than alkali and alkali earth oxides, as well as with respect to lanthana, ceria, zirconia, etc. [45]. In contrast, they are certainly more active in CO_2 adsorption as typical "acidic" oxides such as alumina and titania. This is a reasons for the ability of these zeolites to adsorb reversibly CO_2, thus acting as useful adsorbents for CO_2 capturing and separation [50,51].

3.6 Acido-basic sites of cationic zeolites.

The orthosilicate anion, $[SiO_4]^{4-}$, is a tetrahedral entity assumed to be formed by covalent Si-O bonds. This is associated to the very small size of the Si^{4+} formal cation (0.26 Å radius [52]) and its moderately high charge. According to water solution chemistry, the orthosilicate anion is quite a basic anion, being the conjugated base of a weak acid, orthosilicic acid H_4SiO_4 which is a weak polyprotic acid with $pK_{a1} \sim 9.5$ and $pK_{a4} \sim 19$ [53]. Polymerization and gelling of silicic acid easily occurs. Di-silicic acid is slightly more acidic, but acidity increases significantly with polymerization (pK_a of polysilicic acid is about 6.5 [54]). Thus, orthosilicate anions are quite strong bases, while polysilicate anions are less basic. Conversely, the Al-O bond is essentially ionic, as an effect of its larger ionic radius (0.39 Å for tetrahedral coordination, 0.53 Å for octahedral coordination) and lower charge of Al^{3+} with respect to Si^{4+}. As a result of this, aluminum in its oxides can take tetrahedral,

octahedral coordination or even coordination five, coordination three being also possible [55].

In the case of aluminum silicates, silicate species tend to interact ionically strongly with aluminum ions producing orthosilicate species with oxygen interacting with two Al ions each [56,57]. In these structure, Al coordination is variable, 4, 5 or 6. This occurs also when small amounts of silica are mixed with alumina, forming spinel structures where orthosilicate species occupy tetrahedra of the spinel structure [58]. This shows that the interaction of the silicate with Al ions with ionic bonds is stronger than the interaction between silicate species tending to produce polysilicate species.

Thus, while silica and silicalites (zeolitic silicas) are essentially covalent structures, with low polarity, the structure of zeolites is the more ionic, the more the framework Al content. Thus, alkali zeolites with Si/Al ~ 1, such as LSX (low silica X faujasites) and LTA (Linde type A) zeolites (the richest in Al and alkali), are essentially aluminum,sodium orthosilicates. A similar situation occurs for zeolite Na-X, where Si/Al is 1.2-2. All oxygen atoms in the orthosilicate ions formally bring a net negative charge. These atoms are bridging being actually bonded with a silicon atom through a “covalent” bond, while interacting ionically with a framework aluminum atom and at least one extraframework sodium atom (that frequently interact with more than one oxygen ion). Thus these oxygen atoms certainly possess significant basicity and/or nucleophilicity. On the other hand, being Na zeolite the salts of strong Brønsted acids (the protonic zeolites), they are relatively weak bases.

Additionally, highly uncoordinated sodium ions are also present and interact with these negatively charged oxide species. In spite of the large size and small charge of sodium ions, these ions possess significant Lewis acidity due to the high un-coordination degree. This is shown by the relatively high CO stretching frequency of coordinated carbon monoxide. The Lewis acidity of the Na^+ ions is a very relevant feature for the practical applications of Na-zeolites, including both Na-X and Na-A zeolites, which are reported to be very effective adsorbents for water, CO, H_2S, ammonia, nitriles, nitrogen, which are more or less basic molecules which are supposed to interact predominantly with Na^+ cations. This makes these zeolites active as weak Lewis acid catalysts [37,59].

Sodium cations also cover and mask in part the “basic” oxygen ions thus decreasing their accessibility. This is likely a reason for decreased “kinetic” basicity of these zeolites. On the other hand, the ionic couples between silicate anions and sodium ions (Fig. 10), that may somehow also involve the Lewis acidity of framework Al^{3+}, make Na zeolites acido-

basic solids. This makes them excellent materials for adsorption of CO_2 in the form of carbonate species (see above), as well as for the dissociative adsorption of molecules characterized by protonic acidity such as H_2S [60] and acetic acid [37]. It is very likely that these sites are those active when NaX is used as a “basic” catalyst such as, e.g. for the side-methylation of toluene with methanol [61], for aldol condensation reactions [62] and for dehydrogenations with CO_2 [63].

Cationic zeolites with moderate Si/Al ratio such as Na-MOR or Na-Y faujasite, have obviously a lower density of Na^+ ions and of framework acido-basic sites. This could result in lower activity as adsorbents and catalysts. On the other hand, the occupancy in the cages is also lower, with resulting more space for molecular diffusion and less steric hindrance.

The ionic exchange of Na^+ ions with larger alkali cations, like e.g. Cs^+, which are weaker Lewis acids due to their larger size [44], does increase the basicity of the silicate’s oxide species, which are in fact less perturbed being interacting with less Lewis acidic cations. This effect is, however, to some extent compensated by the increase of steric hindrance for access to these basic sites or even to the overall cavity [64]. In any case the catalytic activity may be enhanced in the case of heavy alkali cationic zeolites such as e.g. Cs faujasites [62,63]. It seems, however, that also these materials are not very strong solid bases.

Cationic zeolites are however apparently good and stable supports for very basic metal oxide or hydroxide catalytic species. This occurs when these cationic zeolites are “overexchanged”, thus containing additional metal oxide species in the cavities. Among others, Cs_2O/CsOH/CsX [65] or KOH/-zeolites [66] are under study for their interesting activity as strong basic catalysts.

Alkali zeolites may also find application in heterogeneous catalysis as supports for other catalytically active phases, such as metals. At least in one case there is already an important application, i.e. the use of Pt/K-LTL catalysts for paraffin aromatization reactions. A catalyst of this type has been developed for the Aromax process (Idemitsu Kosan - Chevron Phillips) to convert C6 – C8 paraffins to benzene [67]. Pt-KL zeolite is also the basic formulation of the catalyst of the RZ platforming process from UOP [68]. This process is a semiregenerative naphtha reforming process, allowing higher aromatics selectivity than other reforming processes with C6 and C7 paraffins as feed [69]. The basicity of KL zeolite is supposed to allow limited coking.

4 Acido-basicity of protonic zeolites.

4.1 Experimental data on the bridging hydroxyl groups.

Protonic zeolites, i.e. those zeolites where the framework charge is balanced, formally, by protons, find industrial applications as acid catalysts in a large number of hydrocarbon conversion reactions. The application of these materials is due to three main properties:

i) the strong Brønsted acidity of bridging Si-(OH)-Al sites generated by the presence of aluminium inside the silicate framework and the balancing proton;

ii) the shape selectivity and confinement effects due to the molecular sieving properties associated to the well-defined crystal pore sizes, where the catalytic active sites are located;

iii) their environmental friendliness, well superior to that of alternative acid catalysts.

The strongly acidic hydroxy groups of zeolites are well characterised by the presence, in the IR spectrum, of moderately sharp and strong bands in the region between 3650 and 3500 cm^{-1} (Fig. 11) as well as by evident ^{1}H MAS NMR peaks in the region 3.6 – 8.0 ppm [70]. With both techniques, it is possible to reveal the acidity of these groups [71]. In fact these spectroscopic signals disappear upon contact with bases like ammonia, pyridines, amines and phosphines, in parallel with the appearance of the features of the corresponding protonated bases. In the presence of weak basic probes (CO, nitriles) a significant perturbation of the spectral characteristics of these groups is evident too.

The position of the IR band due to bridging OH's is somehow dependent on the size of the zeolite cavities, νOH being generally (but not really always) the lower the smaller the cavity. In particular, the OH stretching band position and width can be influenced by weak H-bondings through the cavities [72]. In the case of zeolites with more than one type of quite different cavities, splitting of the band of the bridging hydroxy groups can be observed. Some authors suggested that a correlation exists between OH stretching frequency and the Si-O(H)-Al bond angle [73]. As for ^{1}H MAS NMR peaks of protonic zeolites, the trend among different studies is for increased chemical shift corresponding to an increase in the intrinsic acid strength [74], i.e., protons are more de-shielded in zeolites perceived to be more acidic. On the other hand, the peak position is also sensitive to location: peaks at 3.6–4.3 ppm are due to bridging OH groups in large cages and channels; peaks at 4.6–5.2 ppm to bridging OH groups in small cages of zeolites, while those at 5.2–8.0 ppm are associated to disturbed bridging OH groups interacting with framework oxygen [70]. Parallel ^{1}H NMR and IR studies show that the IR extintion coefficient of the zeolite's bridging OH's is far higher than for silanol groups, and this

allowed Kazansky et al. [75] to propose to use the intensity of the IR band to determine the surface acid strength.

Interestingly, bridging OH's are only detected in the interior of the zeolitic cavities, being the corresponding spectroscopic features (both IR and NMR) absent in any non zeolitic material based on silica and alumina [76] and also on the external surfaces of different zeolites. Thus, the existence of the bridging hydroxy groups Al–(OH)–Si should imply the existence of the cavity. In other words, the cavities (or the microporous zeolitic framework) are possibly involved in the generation and/or stabilization of the bridging OH sites, as well as in the strengthening of their acidity [76].

Besides "zeolitic" bridging OH's, additional OH groups are or may be observed in the case of H-zeolites, as evident in Fig. 11. Terminal silanols similar to those of silica (νOH at 3745$\pm$3 cm^{-1}, ^{1}H NMR signal at 1.2-2.2 ppm) have been found to be located at the external surface, while additional features (νOH at ca. 3780 and 3675 cm^{-1}, ^{1}H NMR signal at 2.4–3.6 ppm) are usually attributed to OH's on extra-framework (EF) alumina or silica-alumina matter. Finally, broad absorptions are also frequently detectable in Al-rich zeolites at lower frequencies (3500-3200 cm^{-1}), likely due to strongly H-bonded OH's in small cavities, such as Al-rich H-FER [77] and H-CHA with Si/Al atomic ratio of 2 [78], but also H-MFI and H-MWW (see Fig. 11).

4.2 Acidity characterization of protonic zeolites by pyridine adsorption

Also in the case of characterization of protonic zeolites, pyridine and CO are the most used molecular probes [32,33]. The spectra of pyridine adsorbed on zeolites (Fig. 12 for HY faujasite with Si/Al ratio = 5 and for Ultra Stable Y faujasite with Si/Al ratio = 30) all present the features of pyridinium ions (in particular the 19a band near 1545 cm^{-1} and the 8a band near 1630 cm^{-1}), as the result of their Brønsted acidity. They also present, after outgassing at r.t., bands of molecular pyridine (in particular the 19b band at 1445-1440 cm^{-1}, together with 8a bands ion the 1600-1595 cm^{-1} region), attributed to H-bonded pyridine. After outgassing at higher temperatures (523 K), the spectra also present, in most cases, the typical features of pyridine bonded to strong Lewis acid sites. In particular, the 19b band of Lewis bonded pyridine is usually ca. 1455-1460 cm^{-1} while the corresponding 8a mode is observed, sometimes split, in the 1610-1624 cm^{-1} range. The position of these bands are similar to those observed on aluminas [55] and on silica-aluminas [79], thus showing that Lewis acidic low-coordination Al^{3+} are available to pyridine adsorption.

The usefulness of the use of pyridine to reveal the acidity of zeolites is somehow hampered by its relatively large size, thus being un-allowed to penetrate small cavities. As said, pyridine cannot enter the LTA zeolite cavities, nor those of chabasites (CHA). As discussed several years ago [80], the size of the cavities of FER zeolite does not allow the easy diffusion of pyridine at room temperature while it does at higher temperatures. Additionally, pyridine does not enter the "side pockets" of the MOR porous structure [81], one of the channels of the BEA structure [82], as well as the sodalite cage and the hexagonal prisms of faujasites [83].

The presence of very small amounts of Lewis sites, if any, is sometimes observed on low-Al content zeolites, and/or for some zeolite structures. The IR spectra of pyridine adsorbed on two protonic faujasite samples (Fig. 12), instead, show, together with features due to protonation of pyridine on the Brønsted acid sites, pyridinium ions, also bands associated to adsorbed molecular pyridine. The couple of bands at 1622-24 and 1452-55 cm^{-1} shows the existence, in both cases, of very strong Lewis acid sites. This is evident for the sample denoted as HY, that certainly contains EF material (OH bands at ca 3675 cm^{-1}, see Fig. 11, and octahedral Al in ^{27}Al MAS NMR spectra). However this is also found (to a slightly lesser extent) for the sample denoted as USY (Ultra-Stable Y), that does not show the features of extra-framework material (see OH bands in Fig. 11) and has quite a high Si/Al ratio (~ 15).

4.3 Adsorption of CO on H-zeolites.

The IR spectra of zeolites upon low temperature CO adsorption are very useful for the characterization of their acidity. In fact, CO as a very weak base interacts through its C atom to the OH's forming a weak hydrogen bond. As a result of this, the OH stretching frequency of the interacting OH's is shifted down with a broadening of the corresponding OH stretching band. In Fig. 13 the spectrum of a typical low Al content protonic zeolite, H-MFI, is reported. By adsorbing CO the most evident interaction is associated to the shift of the bridging OHs stretching band from 3615 to 3304 cm^{-1} ($\Delta\nu$OH 310 cm^{-1}), and to the formation of the CO stretching band at 2175 cm^{-1}. According to the so-called "hydrogen bonding method" arising from the Bellamy-Hallam-Williams relation, the extent of shift down suffered by the νOH band, $\Delta\nu$OH, can be taken as a measure of the strength of the H-bonding interaction, thus giving a measure of the Brønsted acid strength of the surface hydroxyl groups [71]. The data reported in the literature [71,84] indicate that all protonic zeolites have similar Brønsted acidity. Actually, small differences in the $\Delta\nu$OH among

zeolites may arise from additional Van Der Waals interactions as well as from different O-H-(CO) angles caused by the compression of the CO molecule on the opposite walls of the cavities. These effects are possible causes of discrepancy between $\Delta\nu$OHs and CO adsorption enthalpies reported previously [85]. Additionally, as proposed by Chakarova and Hadjiivanov [86,87] the bands of OH groups interacting with CO can also perturbed by Fermi resonances in some zeolites. In any case, the small differences in the $\Delta\nu$OH among zeolites can be not entirely due to different Brønsted OH's acidities. Indeed, most data suggest that the difference in intrinsic Brønsted acid strength of different zeolites is small, if any.

Looking at the νCO region, the spectra also do not allow to distinguish different acid strengths of zeolites OH's. In any case, the CO stretching is observed near 2175-2180 cm^{-1}. However, at least in some cases the spectra show the additional presence of Lewis sites, with additional CO stretching bands in the region 2240-2180 cm^{-1}, where also CO adsorbed on Al^{3+} Lewis sites is usually observed [55]. The feature at 2230 cm^{-1} is particularly evident in the spectrum of CO adsorbed on USY (Fig. 14), in spite of the apparent absence, in this material, of extra-framework matter. The presence of strong Lewis acid sites in this sample is confirmed by the use of other basic probes such as nitriles [83,84].

4.4 Adsorption of CO_2 on protonic zeolites.

As already said, CO_2 is a good probe for surface basicity (nucleophilicity) characterization. In Fig. 9 the spectra of CO_2 adsorbed on H-MOR and Na-MOR samples, both activated under outgassing are shown. Upon adsorption of CO_2 almost no absorption is found to form in the carbonate region on H-MOR, where only a strong band is found near 2360 cm^{-1} whose exceeding intensity saturates the signal but is well evident after outgassing. The shift up agrees with the interaction of CO_2 through one of the oxygen atoms, with the Brønsted acidic OH groups.

This result agrees with literature data showing that CO_2 adsorbs weakly in a molecular way on the hydroxyl groups of porous silicas [88], fully siliceous zeolites [89], high- silica silica-alumina [90] and in other protonic high-silica zeolite such as H-BEA [91] without any formation of carbonate or bicarbonate species. This shows that oxide and hydroxide species of these silica-rich materials, including protonic zeolites, are not significantly basic and nucleophilic.

4.5 Structure and Brønsted acidity of protonic sites of H-zeolites.

All data confirm that the Brønsted acidity of protonic zeolites is due to the bridging OH groups. The spectroscopic data agree suggesting that such acidic protons are actually linked (in the dry zeolite) through a covalent bond to oxygen atoms bridging between a silicon and an aluminum atom. These sites can thus be considered as “perturbed silanol groups”, where an oxygen lone pair interacts with the nearest Al cation through a Lewis base acid bond. This interaction is certainly “favoured” thermodynamically and “exothermic”. However, this interaction is not found (at least to a significant extent) to occur in non-zeolitic mixtures of silica and alumina. In particular, it is sure that the deposition of silicate species on alumina does not give rise to strongly acidic bridging silanols, but only to weakly acidic terminal silanols [92,93]. This is likely due to the stronger stabilization of the silicate species occurring when the silanol stands up on the alumina surface, as a terminal silanol, due to the strong interaction of the three other oxygen atoms with Al ions.

The poor stability of bridging OH’s in alumina-rich environments is also somehow demonstrated by the easy de-alumination of Al-rich zeolites in the protonic form, such as H-X and H-LTA, in contrast to the strong stability of both Al-rich alkali-zeolites (like Na-X and Na-LTA) and the highly siliceous protonic zeolites, as USY, and silicalites too. It can be supposed that the stabilization of the bridging OH’s is associated to the existence of the rigid and highly covalent silica-based zeolite framework, the more, the more silica-rich the framework is. In contrast, the Al coordination in silicoaluminates is flexible and variable, where coordination 4, 5 and 6 are allowed and well characterized. The evident weak interactions of the proton of bridging OH’s with the other oxygen atoms exposed on the zeolite cavities may also give a stabilizing contribution.

The strong protonic activity of the sites is likely associated to several factors. The hydrogen bonding activity (occurring without a real proton jump, as when interacting with CO) of bridging silanols is strongly increased by the interaction of the OH with the aluminum ion, that makes the hydroxyl group bridged and the proton more cationic. On the other hand, the strength of Brønsted acid sites is the stronger, the more the deprotonated anionic site is stabilized and the more the protonated base is stabilized too. One of the reasons for high acidity of protonic centers in zeolites is associated to the stabilization of the protonated molecules by the “tridimensional solvation” occurring in the zeolite cages by the Van der Waals interactions with the walls of the cavities, i.e. with the siloxane bridges

(Fig. 15). This differentiates microporous materials from normal porous or mesoporous surfaces, where these solvation effects are certainly weaker.

The stabilization of the framework, arising from the much stronger interaction of the Al^{3+} ions with the dissociated silicate species than with the undissociated silanol, is certainly a way to stabilize the system after proton jump. On the other hand, the negative charge formally formed on the silicate's oxygen upon proton jump may be somehow "delocalized" on the four nearly equivalent oxygen atoms surrounding the Al cation.

Several papers report on the stronger Brønsted acidity of silica-rich protonic zeolites with respect to alumina-rich protonic zeolites [94]. In parallel, it has been reported that silanols of silica (pK_{a1} ~ 4.5-7) and of polysilicic acids (pK_{a1} ~ 6.5) are definitely stronger than those of pyrosilic (or disilicic) acid (pK_{a1} ~ 9.5) and orthosilicic (pK_{a1} ~ 9.5) acid [95,96]. This can be explained by the delocalization of the negative charge of the dissociated species over S-O-Si siloxane bonds. In fact, siloxane groups, whose bond angle is very flexible in contrast to the O-Si-O bond angle that is not, have some character of "double bond" which is associated to an hyper-conjugation effect, i.e. the $n_O \rightarrow \sigma^*_{Si\text{-}O}$(vicinal) interaction, a bonding interaction between an oxygen lone pair and the antibonding orbital of the vicinal Si-O bond [97,98]. These interactions can allow the delocalization of the terminal anionic charge of a silicate species ($Si\text{-}O^-$) over the siloxane bridges, the more the larger is the polysilicate entity. This effect can explain the slightly stronger acidity of low Al-content zeolites with respect to zeolites richer in Al. This phenomenon, with the delocalization of the negative charge on the siloxane oxygens of the cavities, also explains why the zeolite cavities may act as stabilizing environments for protonated cationic species.

On the other hand, it must be also considered that the molecular traffic may be more hindered on zeolites richer in protons with respect to zeolites with less protons, due to the strong interaction of molecules with more adsorbing sites. This might result in lower catalytic activity even if the acidity is not weaker [99].

4.6 The Lewis acidity of protonic zeolites

Lewis acidity in protonic zeolite is due to available coordinatively unsaturated Al^{3+} ions, as shown by the adsorption of pyridine and carbon monoxide. Studies using hindered probe molecules demonstrated that Lewis acid sites occur or may occur at the external surface of zeolites, where the "zeolitic" structure in some way vanishes [83]. Additionally, Lewis acidity frequently comes from "extraframework" matter, composed by alumina-like or silica-alumina-like debris. In fact, protonic zeolite catalysts may contain, as a result of the

preparation, or of an intentional pretreatment, significant amounts of species external to the framework. Several zeolites are actually applied after treatments tending to increase their stability and also, in case, to further enhance surface acidity and shape selectivity effects. These treatments, like steam dealumination, can cause the decrease of the framework Al content and the release from the framework of aluminum-containing species that contribute in stabilizing the framework, but can also contain additional catalytically active acid sites. These particles can also narrow the size of the zeolite channels or of their mouths, thus improving the shape selectivity effects. Extraframework material is composed by very small particles mostly containing Al cations complexed by oxide ions and/or OH's but sometimes also involving silicate species, likely interacting with the framework walls, located in the cavities or on the external surface. As said, the presence of EF gives rise to the presence of strong additional bands in the IR OH stretching, usually above 3750 cm^{-1} and in the region 3730-3650 cm^{-1} (see Fig. 11 for samples H-MFI (30) and HY (5)). These species are also responsible for ^{1}H NMR peaks at -0.5- + 0.7 and 1.7-2.7 ppm [70] and reveal medium-strong Brønsted acidity. Similarly, the detection of octahedral Al ions in ^{27}Al NMR techniques is evidence of EF. EF species usually contain exposed Al ions acting as strong Lewis acid sites.

Recently, it has been pointed out the possible activity of framework Al ions as Lewis acid sites [84]. In fact, it is well-known that Al^{3+} can easily take coordination four, five, and six, his preferred coordination being most commonly six. Al ions are exclusively octahedrally coordinated in all Al hydroxides and oxyhydroxides and in the thermodynamically stable phase of alumina (α-Al_2O_3, corundum). It is also predominantly coordinated six in all other alumina polymorphs [55]. Penta- and hexa- coordinated aluminium ions are present in several alumino-silicates as well as in amorphous silica-alumina [56]. In aluminosilicate glasses Al takes mostly a tetrahedral coordination, as in zeolites, but this also depends on the amount of balancing cations and also on the metals involved [100]. On the other hand, it has been shown that the energy difference between tetrahedral and octahedral Al coordination is small enough to allow for their interconversion [101]. Several studies report of a quite easy and reversible conversion of framework tetrahedral Al ions to octahedral coordination in conditions close to those of dealumination of faujasite zeolites [102,103,104]. It seems likely that Al ions can behave as other cations do, in framework positions in zeolites. This is the case e.g. of Ti^{4+} in Ti silicalite TS-1 [105] as well as of Sn^{4+} and other cations, that behave as Lewis acids when in substitutional positions in silicalites [106].

However, it is normally supposed that the access of basic molecules to the framework Al^{3+} ions does not occur mainly because it is hindered by, or competes with, the interaction of the base with the near proton (Fig. 16).

Nevertheless, in complex pore zeolites it is possible that Al ions can interact with basic molecules when the proton is in position internal to another cavity. This is the case, e.g., of USY faujasite, where it has been proposed [84] that framework Al ions can be active in adsorbing bases from the supercage when they are associated to protons located in the sodalite cavity or in the hexagonal prism. Tetrahedral framework Al ions can enlarge their coordination to five, without any dehydration, by reacting with a base from the other side with respect that where the acidic OH lays. This interaction would also modify the state of the bridging hydroxyl group whose OH stretching mode will be perturbed. In fact it has been shown that when the base adsorbed is quite strong, such as pyridine, the LF (Low Frequency) OH stretching band (ca 3550 cm^{-1}, due to OH's located in the sodalite cage, in position O2 (Fig.s 1 and 17) broadens very much and shifts, to be not well distinguishable from the other OH absorptions. When the probe has intermediate basicity, i.e. in the case of pivalonitrile, this band is shifted to 3480 cm^{-1}, $\Delta\nu \approx 80$ cm^{-1}. Instead, when the interaction involves CO, thus being essentially more a polarization than a real additional coordination [107], the perturbation of the OH band is negligible. The situation of low-Al Y zeolite is not common to other zeolites such as H-MFI, where protons are supposed to point entirely towards the channels where molecule can diffuse, thus hindering and competing with the access of bases to the Al ions. However, other zeolites can present a similar situation such as, e.g. H-MCM-22 (H-MWW) where two families of accessible cavities exist. In fact, studies of the adsorption of probe molecules suggest that also in this case framework Lewis acidity may exist [108]. Indeed the presence of the broad OH stretching bands atv 3500-3200 cm^{-1} observed in some Al-rich zeolites (Fig. 11) is attributed to protons in the small cavities of zeolites, that may correspond to Al ions that can be attacked from the side of the larger cavities.

These data and our interpretations suggest that also extraframework material-free (or nearly free) high silica zeolites may display Lewis acidity and could act as Lewis acid catalysts, due to the activity of framework Al atoms. It has been reported, in particular, that the sample USY (30), an ultra-stable dealuminated Y faujasite, is an excellent catalyst for some fine chemistry reactions most typically catalyzed by homogenous Lewis acids [109].

It can be remarked that the evident band of adsorbed CO at 2230 cm^{-1}, attributed to the interaction of CO with framework Al ions from the supercage side, is not observed in the

case of HY(5). This can be interpreted as an evidence of a role of this site for the formation or anchoring of extraframework species. It is possible that extraframework alumina particles just form and anchor on the supercage wall on the most reactive sites, where such framework Al ions, available to expand their coordination sphere, are located.

4.7 Structural effects in catalysis on protonic zeolites.

The relations between structural parameters and acid strength of hydroxyl groups of zeolites have been object of many discussions. Sastre, Niwa and coworkers concluded that a complex mixture of short- and long-range factors is at play [110]. Its seems quite established today that protonic zeolites have very similar Brønsted acid strengths, with a relevant role of local geometric factors differentiating their behavior [111]. Experimental, as well as theoretical, data show that, besides the interactions of the functional groups of the reactive molecules with the zeolites Brønsted sites, the van der Waals interactions of other unreactive groups of atoms with the zeolite cavity walls may be very relevant and stabilize the intermediates. These interactions may vary significantly as a function of the type of the zeolite, the dimension and shape of the cavities as well as the Al and proton content and the presence of EF. Also, they depend on the size and shape of the molecule. These "confinement effects" make the cavities of the single zeolite structures unique solvation and reactivity environments and play relevant role in the catalysis by zeolites [112]. Different catalytic activities would predominantly reflect differences in the size and solvating properties (confinement effect) of their cavities, rather than differences in acid strength [113,114]. As it is well known, shape selectivity is a key phenomenon making forbidden (or strongly inhibited) reactions involving transition states, intermediates and/or products whose size exceeds that of the catalyst cavities [115,116], thus somehow favouring competitive reactions. In contrast, confinement effects can directly favour reactions whose transition states match the cavity size and are stabilized by the cavity [99,117].

An example of "positive" confinement effects is the easy formation of aromatics, such as benzene, toluene and styrene, and the relatively low coking rate occurring on medium-pore zeolites such as H-MFI and LTL, from a number of reactants such as light paraffins and olefins, methanol, ethanol, vegetable oils, etc. This behaviour, differentiating medium pore zeolites from small pore zeolites and large pore zeolites, could be associated to the optimal size of the cavity for cyclization reactions but too small for extensive coking.

5. Conclusions.

The spectroscopic features characterizing cationic zeolites and protonic zeolites have been reviewed and discussed critically. Cationic zeolites with Si/Al ratio ~ 1, such as Na-LSX, Na-X and Na-LTA are constituted by orthosilicate species characterized by relevant basicity, ionically interacting with framework tetrahedrally-coordinated Al ions and extraframework Na ions. They contain a large amount of acid-base sites, whose access is, however, highly hindered. The exchange with heavier alkali ions such as Cs increases slightly the basic nature of these sites but also makes more hindered molecular diffusion. Cationic zeolites with higher Si/Al ratios have less active sites but less hindered molecular diffusion. These solids have strong ionicity and moderate acido-basicity, making them excellent regenerable adsorbents for polar molecules, acting also as molecular sieves due to the different size of the cavities and windows. However, their basicity is moderate, and their catalytic activity as basic catalysts is also moderate.

Protonic zeolites are stable only when their Si/Al atomic ratio is relatively high, to prevent easy dealumination. The strong acidity of the bridging hydroxyl groups is associated to the ability of Si-O-Si bridges in polysiloxane species to stabilize the anionic charge arising from its dissociation and the ability of the zeolitic cages where these oxygen atoms are exposed to stabilize the cationic charge of the protonated molecules.

Figure Captions.

Fig. 1. The structure of Na-faujasite Na-X.

Fig. 2. The structure of zeolite Na-A (Na-LTA).

Fig. 3. The structure of zeolite Na-MOR.

Fig. 4. FT-IR spectra of pyridine adsorbed on NaX zeolite after previous activation at 773 K, contact at r.t. (10 Torr) and outgassing at increasing temperatures (300-573 K).

Fig. 5: FT-IR spectra of activated NaX in the presence of CO gas under evacuation at 163K (a), 173K (b), 183 K (c), 193 K (d), 203 (e) and 213 K (f) in the CO stretching range

Fig. 6. FT-IR spectra of CO adsorbed at low temperature on Na-MOR (right) and Na-LTA (left). The strongest spectra are recorded at 133 K in the presence of the gas (10 Torr). The other spectra are recorded upon warming under outgassing up to 250 K. In the insets, the amplifications of the spectra recorded after outgassing at 180 K and 223 K (lower spectrum for Na-LTA, right).

Fig. 7. FT-IR spectra of the species arising from CO_2 adsorption on NaX zeolite after previous activation at 773 K. Full heavy line: in contact with the gas at room temperature. Broken and thin full line: after brief evacuation and after outgassing up to 10^{-2} torr, at r.t.,. respectively.

Fig. 8. FT-IR spectra of the species arising from CO_2 adsorption on NaA zeolite after previous activation at 773 K. Full heavy line: in contact with the gas at room temperature. Broken and thin full line: after brief evacuation and after outgassing up to 10^{-2} torr, at r.t., respectively.

Fig. 9. FT-IR spectra of the species arising from CO_2 adsorption on H-MOR and Na-MOR zeolites after previous activation at 773 K, recorded in contact with CO_2, 10 Torr at r.t..

Fig.10. A representation of the acid-basic site in Na-zeolites.

Fig. 11. FT-IR spectra of the zeolite samples after activation by outgassing at 773K. The number in parenthesis is the Si/Al ratio. The dashed lines provide evidence of broad absorptions in the spectra.

Fig. 12. FT-IR spectra of pyridine adsorbed on two protonic faujasite samples, after previous activation at 773 K, contact at r.t. (10 Torr) and outgassing at increasing temperatures (300-573 K).

Fig. 13. FT-IR spectra of H-MFI (50): activated at 773 K and cooled at 130 K (dotted line), after saturation with CO at 130 K (gray line) and outgassing at increasing temperatures (from top) in the range 130–180 K.

Fig. 14. FT-IR spectra of CO adsorbed at 130K on two protonic faujasite samples (after activation by outgassing at 773K) followed by outgassing upon warming at increasing temperature until 200K.

Fig. 15. Adsorption of pyridine on Brønsted acid sites of zeolites: concept scheme.

Fig. 16. Adsorption of pyridine on framework Lewis acid site of USY faujasite zeolite: concept scheme.

References

[1] M. Guisnet, J.P. Gilson, eds., Zeolites for Cleaner Technologies, Imperial College Press 2002

[2] W. Vermeiren, J.P. Gilson, Top. Catal. 52 (2009) 1131-1161

[3] C. Martínez, A. Corma, Coord.. Chem. Rev. 255 (2011) 1558–1580

[4] A. Primo, H. Garcia, Chem. Soc. Rev. 43 (2014) 7548-7561

[5] G. Busca, Heterogeneous Catalytic Materials, Elsevier, 2014, pp. 197-250.

[6] A.M. Beale, F. Gao, I. Lezcano-Gonzalez, C.H.F. Peden, J. Szanyi, Chem. Soc. Rev.44 (2015) 7371-7405

[7] R. Zhang, N. Liu, Z. Lei, B. Chen, Chem. Rev. 116 (2016) 3658−3721

[8] D. Pietrogiacomi, M.C. Campa, M. Occhiuzzi, Catal. Today 227 (2014) 116–122

[9] M. Tagliabue, D. Farrusseng, S. Valencia, S. Aguado, U. Ravon, C. Rizzo, A. Corma, C. Mirodatos, Chem. Eng. J. 155 (2009) 553–566

[10] B. Sreenivasulu, I. Sreedhar, Environ. Sci. Technol. 49 (2015) 12641−12661.

[11] N. Kosinov, J. Gascon, F. Kapteijn, E.J.M. Hensen, J. Membr. Sci. 499 (2016) 65-79

[12] S. Cinar, B. Beler-Bayka,l Water Sci Technol. 51(2005) 71-77.

[13] D. Barthomeuf, Catal. Rev. Sci. Eng., 38 (1996) 521-612

[14] J. Weitkamp, M. Hunger, Stud. Surface Sci. Catal., 168 (2007) 787-835.

[15] G. Busca, Ind. Eng. Chem. Res., 48 (2009) 6486–6511

[16] Y. Ono, H. Hattori, Solid Base Catalysis, Springer (2011) pp. 170-178.

[17] T. Ennaert, J. Van Aelst, J. Dijkmans, R. De Clercq, W. Schutyser, M. Dusselier, D. Verboekend, B.F. Sels, Chem. Soc. Rev., 45 (2016) 584-611

[18] J.-L. Berchot, D. Vivien, D. Gourier, J. Thery, R. Collongues, J. Solid State Chem. 34 (1980) 199-205

[19] I. Ponsot, G. Dal Mas, E. Bernardo, R. Dal Maschio, V. M. Sglavo, J. Ceram. Proc. Res. 15 (2014)411-417 (2014)

[20] Y. Xiang, J. Du, M.M. Smedskjaer, J.C. Mauro, J. Chem. Phys. 139 (2013) 044507.

[21] A.V. Larin, Phys Chem Minerals 40 (2013) 771–780

[22] T. Frising, P. Leflaive, Micropor. Mesopor. Mater. 114 (2008) 27-63.

[23] F. F. Porcher, M. Souhassou, C. E. P. Lecomte, Phys. Chem. Chem. Phys., 16 (2014) 12228--12236

[24] A. Goursot, V. Vasilyev, A. Arbuznikov, J. Phys. Chem. B 101 (1997) 6420-6428.

[25] R. Arletti, L. Gigli, F. Di Renzo, S. Quarteri, Micropor. Mesopor. Mat. 228 (2016) 248-255.

[26] D. A. Faux, W. Smith, and T. R. Forester, J. Phys. Chem. B 101 (1997) 1762-1768

[27] A. Alberti, P. Davoli, G. Vezzalini, Z. Kristallogr. 175 (1986) 249-259.

[28] S. Devantour, A. Abdoulaye, J.C. Giuntini, F. Henn, J. Phys. Chem. B, 105 (2001) 9297-9301

[29] G. Maurin, P. Senet, S. Devantour, F. Henn, J.C. Giuntini, J. non-Crist. Solids, 307-310 (2002) 1050-1054.

[30] R.G. Bell, S. Devautour, F. Henn, J.C. Giuntini, J. Phys. Chem. B 2004, 108, 3739-3745.

[31] G. Busca, Catal. Today 41 (1998) 191-206.

[32] G. Busca, in “Metal Oxides: chemistry and applications”, J.L.G. Fierro editor, CRC Press, Boca Raton, Fla., USA, 2005, pag. 247-318.

[33] S. Bordiga, C. Lamberti, F. Bonino, A. F. Thibault-Starzyk, Chem. Soc. Rev., 44(2015) 7262-7341

[34] T. Wroblewski, L. Ziemczonek, G. P. Karwasz, Czech. J. Phys. 54 (2004) C747-C752.

[35] T.D. Klots, Spectrochim. Acta Part A 54 (1998) 1481-1498.

[36] R. Ferwerda, J.H. van der Maas, P.J. Hendra, J. Phys. Chem. 97 (1993) 7331-7336.

[37] T.K. Phung, M.M. Carnasciali, E. Finocchio, G., Busca, Appl. Catal. A: Gen. 470 (2014) 72-80

[38] T. Montanari, P. Kozyra, I. Salla, J. Datka, P. Salagre, G. Busca J. Mater. Chem. 16 (2006) 995-1000.

[39] G. Martra, R. Ocule, L. Marchese, G. Centi and S. Coluccia, Catal. Today 2002, 73, 83-93.

[40] S. Bordiga, C. Lamberti, F. Geobaldo, A. Zecchina, G. Turnes Palomino, C. Otero Areán, Langmuir, 11 (1995) 527.

[41] O. Marie, P. Massiani and F. Thibault-Starzyk, J. Phys. Chem. B, 108 (2004) 5073.

[42] I. Salla, T. Montanari, P. Salagre, Y. Cesteros, G. Busca, J. Phys. Chem. B 109 (2005) 915.

[43] E. Garrone, R. Bulánek, K. Frolich, C. Otero-Areán, M. Rodríguez Delgado, G. Turnes Palomino, D. Nachtigallová, P. Nachtigall, J. Phys. Chem. B, 110 (2006) 22542.

[44] I. Salla, T. Montanari, P. Salagre, Y. Cesteros, G. Busca, Phys. Chem. Chem. Phys. 7 (2005) 2526.

[45] G. Busca, Chem. Rev. 110 (2010) 2217-2249.

[46] G. Herzberg Molecular Spectra and Molecular Structure, van Nostrand Reinhold, New York, 1950.

[47] S. Coluccia, L. Marchese, G. Martra, Micropor. Mesopor. Mat. 30 (1999) 43-56.

[48] G. Ramis, G. Busca, V. Lorenzelli, Mater. Chem. Phys., 29 (1991) 425-435.

[49] D.H. Gibson, Coord. Chem. Rev., 185–186 (1999) 335-355.

[50] T. Montanari, G. Busca, Vibrational Spectroscopy, 46 (2008) 45-51.

[51] T. Montanari, E. Finocchio, E. Salvatore, G. Garuti, A. Giordano, C. Pistarino, G. Busca, Energy, 36 (2011) 314-319.

[52] R.D. Shannon, C.T. Prewitt, Acta Cryst. B25 (1969) 925-945

[53] J.L. Provis, in J.L. Provis, J.S.J. Van Deventer, eds., Geopolymers, structure, processing, properties and industrial applications, CRC Press, 2009, p. 50-71.

[54] J. Miñones, O. Conde, Colloid & Polymer Sci. 266 (1988) 353-358

[55] G. Busca, Advan. Catal., 57 (2014) 319-404

[56] D.T. Griffen, Silicate Crystal Chemistry, Oxford University Press, 1992

[57] S. Aryal, P. Rulis, W.Y. Ching, Amer. Min. 93 (2008) 114-123,

[58] A. K. Chakraborty, J. Am. Ceram. Soc. 62 (1979) 120–124

[59] N. Nagaraju, P. Mehboob, Ind. J. Chem. Tech. 3 (1996) 253-255

[60] H.G. Karge, R. János, J. Colloid Interf. Sci. 64 (1978) 522-532.

[61] J.M. Serra, A. Corma, D. Farrusseng, L. Baumes, C. Mirodatos, C. Flego, C. Perego, Catal. Today 81 (2003) 425–436.

[62] J. Li, J- Tai, R.J. Davis, Catal. Today 116 (2006) 226-233.

[63] G. Zhao, H. Chen, J. Li, Q. Wang, Y. Wang, S. Ma, Z. Zhu, RSC Adv., 5 (2015) 75787–75793

[64] T. Montanari, I. Salla, G. Busca, Micropor. Mesopor. Materials, 109 (2008) 216-222

[65] H. Han, M. Liu, F. Ding, Y. Wang, X. Guo, C. Song, Ind. Eng. Chem. Res. 55 (2016) 1849−1858

[66] W. Xu, S. Ji, W. Quan, J. Yu, Mod. Res. Catal., 2 (2013) 22-27

[67] T. Fukunaga, H. Katsuno Catal. Surv. Asia 14 (2010) 96–102

[68] G. J. Antos, M. D. Moser, M. P. Lapinski, in Catalytic Naphtha Reforming: 2nd Ed., ed. by G.J. Antos, A.M. Aitani, Dekker. New York, 2004, pp. 335-352.

[69] M. Lapinski, L. Baird, R. James, in R.A. Meyers ed. Handbook of petroleum refining processes, 3rd ed., Mc Graw Hill, 2006, p. 4.3-31.

[70] Y. Jiang, J. Huang, W. Dai, M. Hunger, Solid State Nucl. Magn. Res. 39 (2011) 116-141.

[71] K.I. Hadjiivanov, Advan. Catal. 57 (2014) 99-3128.

[72] U. Eichler, M. Brändle, J. Sauer, J. Phys. Chem. B, **,** 101 (1997) 10035-10050.

[73] K.P. Schroder, J. Sauer, M. Leslie, C.R.A. Catlow, J.M. Thomas, Chem. Phys. Lett. 188 (1992) 320-325.

[74] A. Simperler, R. G. Bell, M. W. Anderson, J. Phys. Chem. B. 108 (2004) 7142-7151.

[75] V.B. Kazansky, A.I. Seryk, V. Semmer-Herledan, J.Fraissard, Phys. Chem. Chem. Phys. 5 (2003) 966-969.

[76] M. Bevilacqua, T. Montanari, E. Finocchio, G. Busca, Catal. Today*,* 116 (2006) 132-142

[77] L. Domokos, L. Lefferts, K. Seshan, J.A. Lercher, J. Mol. Catal. A: Chem., 162 (2000) 147-157.

[78] L. Regli, A. Zecchina, J. G. Vitillo, D. Cocina, G. Spoto, C. Lamberti, K.P. Lillerud, U. Olsbye, S. Bordiga, Phys. Chem. Chem. Phys., 7 (2005) 3197-3203.

[79] T.K.Phung. G. Busca, Catal. Commun. 68 (2015) 110–115

[80] M. Trombetta, G. Busca, J. Catal. 187 (1999) 521-523.

[81] M. Bevilacqua, A. Gutièrrez Alejandre, C. Resini, M. Casagrande, J. Ramirez and G. Busca, Phys. Chem. Chem. Phys. 4 (2002) 4575-4583.

[82] M. Trombetta, G. Busca, L. Storaro, M. Lenarda, M. Casagrande, A. Zambon, Phys. Chem. Chem. Phys., 2 (2000) 3529-3537

[83] T. Montanari, E. Finocchio, G. Busca, J. Phys. Chem. C, 115 (2011) 937–943

[84] T. K. Phung, G. Busca, Appl. Catal. A: Gen., 504 (2015) 151-157.

[85] C. Otero Arean, M. R. Delgado, P.Nachtigall, Ho Viet Thang, M.Rubes, R. Bulanek, P. Chlubna-Eliasova, Phys. Chem. Chem. Phys., 16 (2014) 10129-10141.

[86] K. Chakarova, K. Hadjiivanov, Chem. Commun. 47 (2011) 1878–1880

[87] K. Chakarova, K. Hadjiivanov, Micropor. Mesopor. Mater. 177 (2013) 59–65.

[88] T.-L. Chew, A. L. Ahmad, S. Bhatia, Advan. Colloid Interf. Sci. 153 (2010) 43–57

[89] T. D. Pham, R. Xiong, S. I. Sandler, R. F. Lobo, Micropor. Mesopor. Mater. 185 (2014) 157–166

[90] J.B. Peri, J. Phys. Chem. 72 (1968) 2917-2925.

[91] M.R. Delgado, C. Otero Arean, Energy 36 (2011) 5286-5291

[92] E. Finocchio, G. Busca, S. Rossini, U. Cornaro, V. Piccoli, R. Miglio, Catal Today 33 (1997) 335-352.

[93] A. R. Mouat, C. George, T. Kobayashi, M. Pruski, R.P. van Duyne, T.J. Marks, P.C. Stair, Angew. Chem. Int. Ed. 54 (2015)13346 –13351.

[94] D. Bartohomeuf, Mater. Chem. Phys. 17 (1987) 49-55.

[95] J. A. Tossell, N. Sahai, Geochimica et Cosmochimica Acta, Vol. 64, No. 24, pp. 4097– 4113, 2000

[96] M. Sulpizi, M.-P. Gaigeot, M. Sprik, J. Chem. Theory Comput. 2012, 8, 1037−1047

[97] J. Passmore, J.M. Rautiainen, Europ. J.Inorg. Chem. (2012) 6001-6010.

[98] F. Weinhold, R. West, J. Am. Chem. Soc., 135 (2013) pp 5762–5767

[99] T.K. Phung, L. Proietti Hernández, A. Lagazzo, G. Busca, Appl. Catal. A: Gen., 493 (2015) 77-89

[100] J. F. Stebbins, S. Kroeker, S. K. Lee, T.J. Kiczenski, J. Non-Cryst. Solids 275 (2000) 1-6.

[101] L.J. Criscenti, S.L. Brantley, K. T. Mueller, N. Tsomaia, J.D. Kubicki, Geochim. Cosmochim. Acta, 69 (2005) 2205–2220.

[102] B.H. Wouters, T.H. Chen, P.J. Grobet, J. Am. Chem. Soc. 120 (1998) 11419-11425.

[103] A. Omegna, R. Prins, J.A. van Bokhoven, J. Phys. Chem. B 109 (2005) 9280-9283.

[104] Z. Yan, D. Ma, J. Zhuang, X. Liu, X. Liu, X. Han, X. Bao, F. Chang, L.Xu, Z. Liu, J. Mol. Catal. A: Chem.194 (2003) 153–167

[105] E. Astorino, J. Peri, R.J. Willey, G. Busca, J. Catal. 157 (1995) 482-500

[106] M. Moliner, Dalton Trans. 43 (2014) 4197-4208.

[107] F. Leydier, C. Chizallet, D. Costa, P. Raybaud, Chem. Commun., 48 (2012) 4076-4078

[108] M. Bevilacqua, D. Meloni, F. Sini, R. Monaci, T. Montanari, G. Busca, J. Phys. Chem. C 112 (2008) 9023–9033.

[109] R.A. Sheldon, I., Arends, U., Hanefeld, Green Chemistry and Catalysis, Wiley, Weinheim, 2007, 59-60.

[110] G. Sastre, N. Katada, M. Niwa, J. Phys. Chem. C, 114 (2010) 15424–15431

[111] B. Xu, C. Sievers, S.B. Hong, R. Prins, J.A. van Bokhoven, J. Catal. 244 (2006) 163-168

[112] R. Gounder, E. Iglesia, Angew. Chem. Int. Ed. 49 (2010) 808 –811

[113] R. Gounder, A. J. Jones, R. T. Carr, E. Iglesia J. Catal. 286 (2012) 214–223

[114] D.A. Simonetti, R.T. Carr, E. Iglesia, J. Catal. 285 (2012) 19-30

[115] P.B. Weisz V.J. Frilette, J. Phys. Chem. 64 (1960) 382-382.

[116] B. Smit, T.L.M. Maesen, Nature 451 (2008) 671-678.

[117] R. Gounder, E. Iglesia, Acc. Chem. Res. 45 (2012) 229-238.

Figure(s)

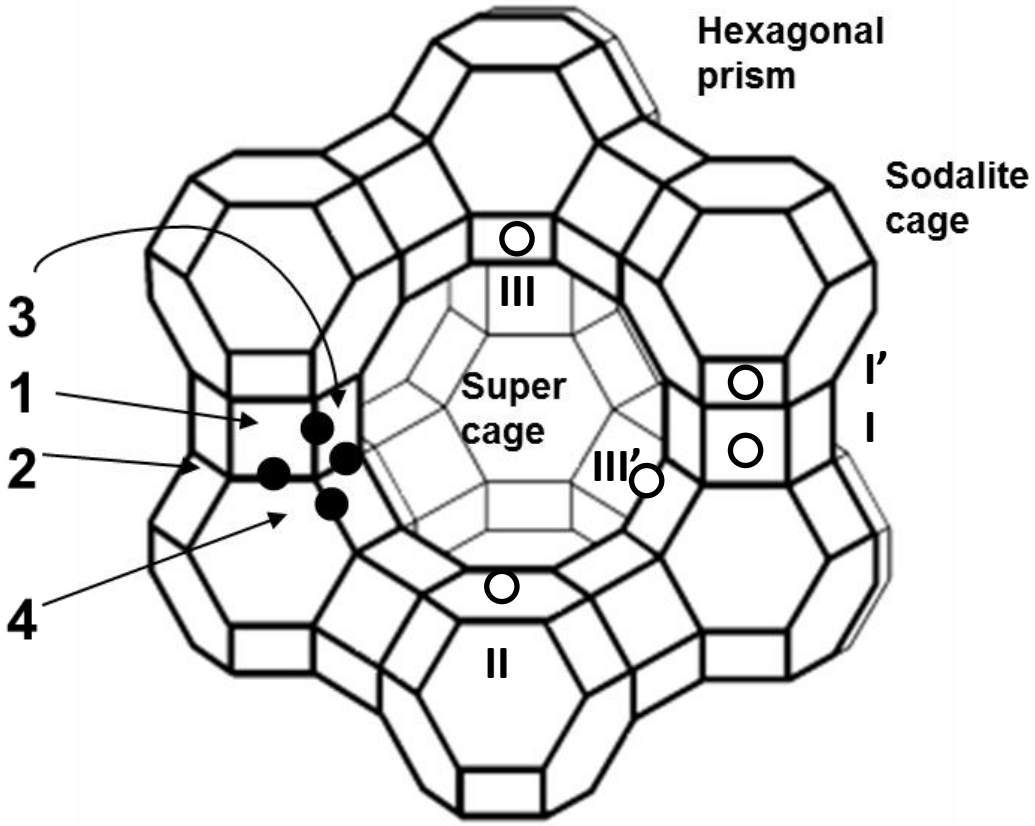

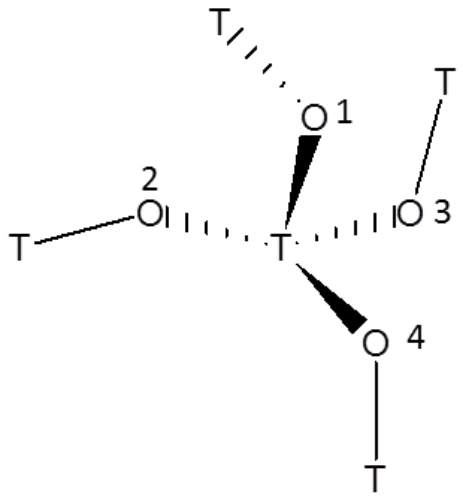

● oxygen
○ sodium

Figure 1

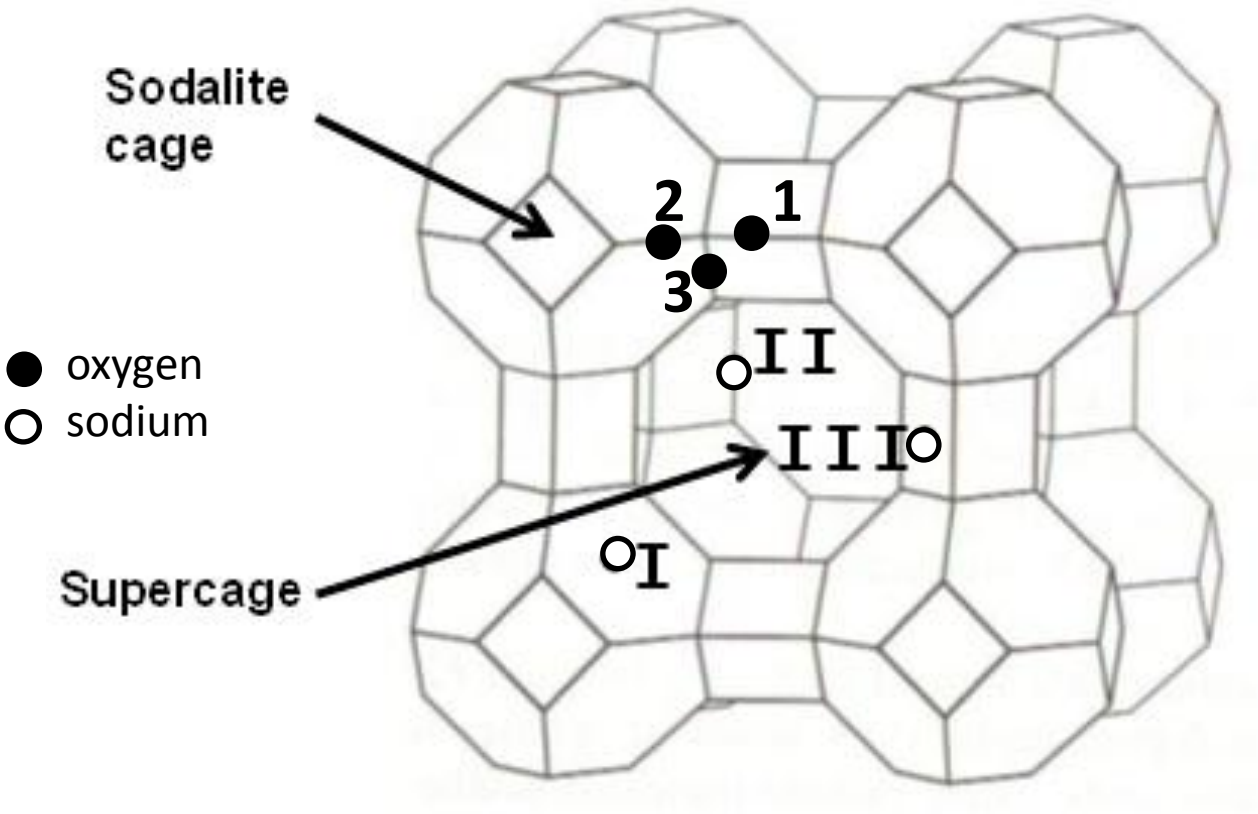

Figure 2

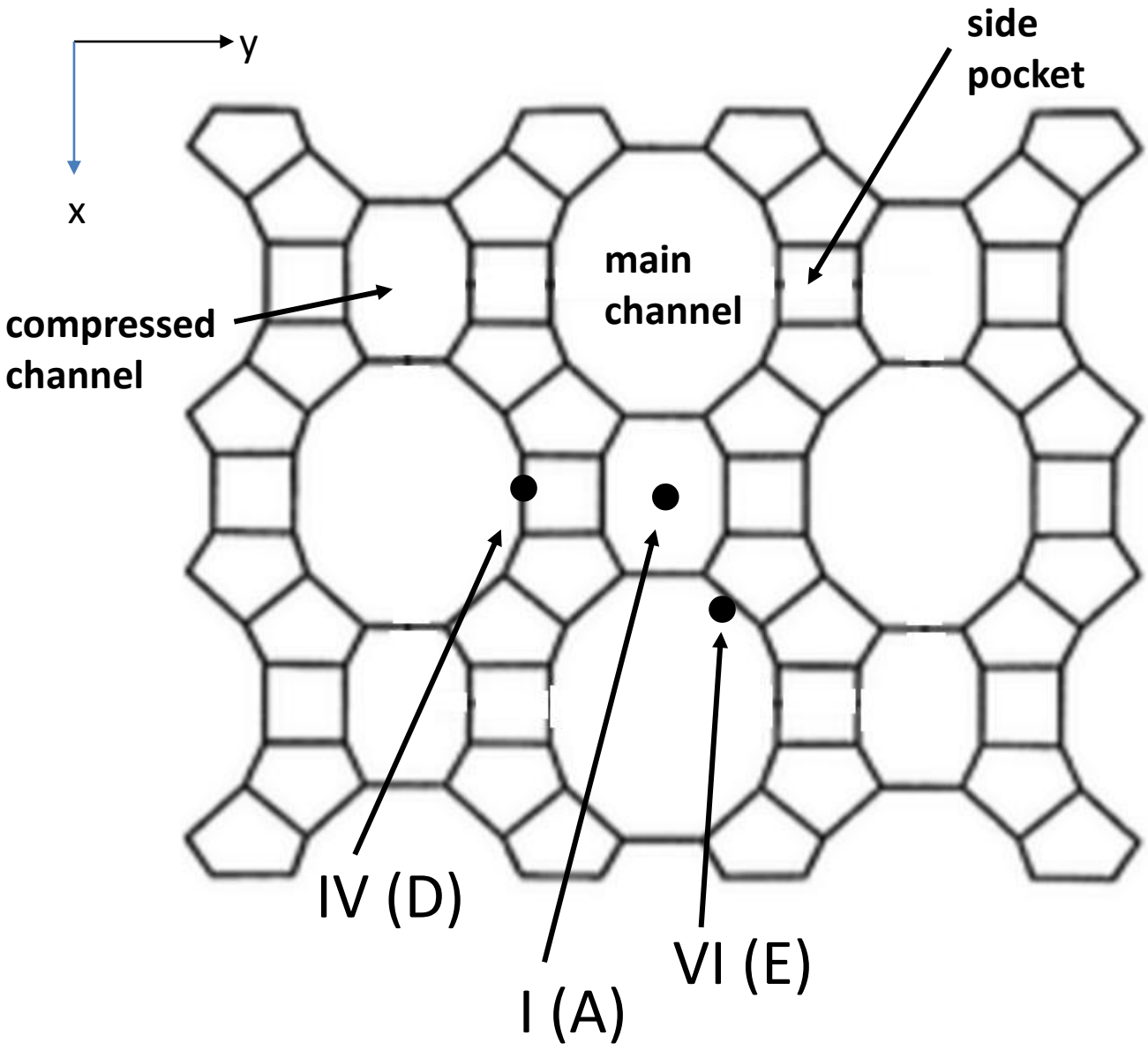

Figure 3

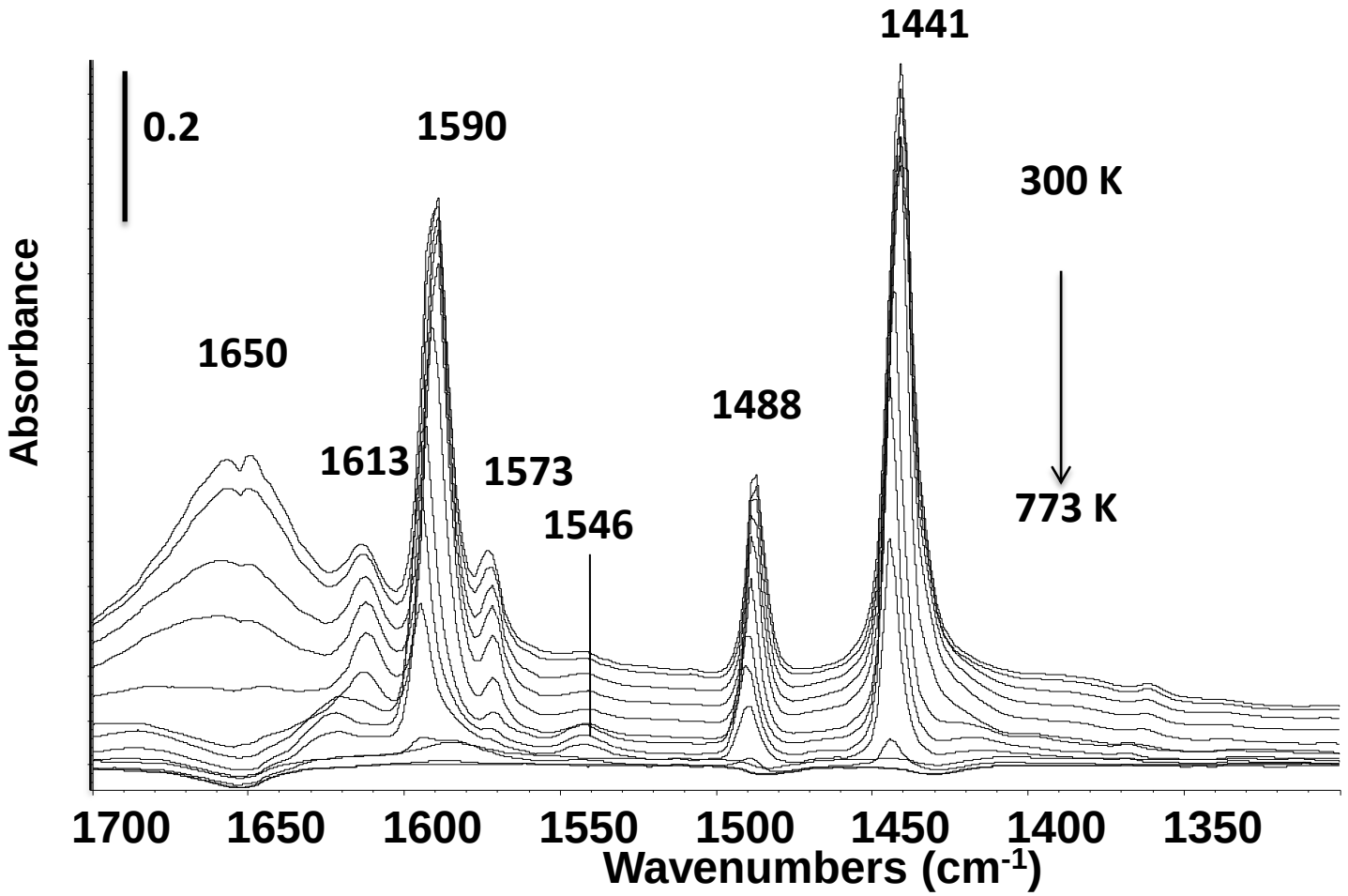
1441
0.2
1590
300 K
Absorbance
1650
1488
1613
1573
773 K
1546
1700
1650
1600
1550
1500
1450
1400
1350
Wavenumbers (cm-1)

Figure 4

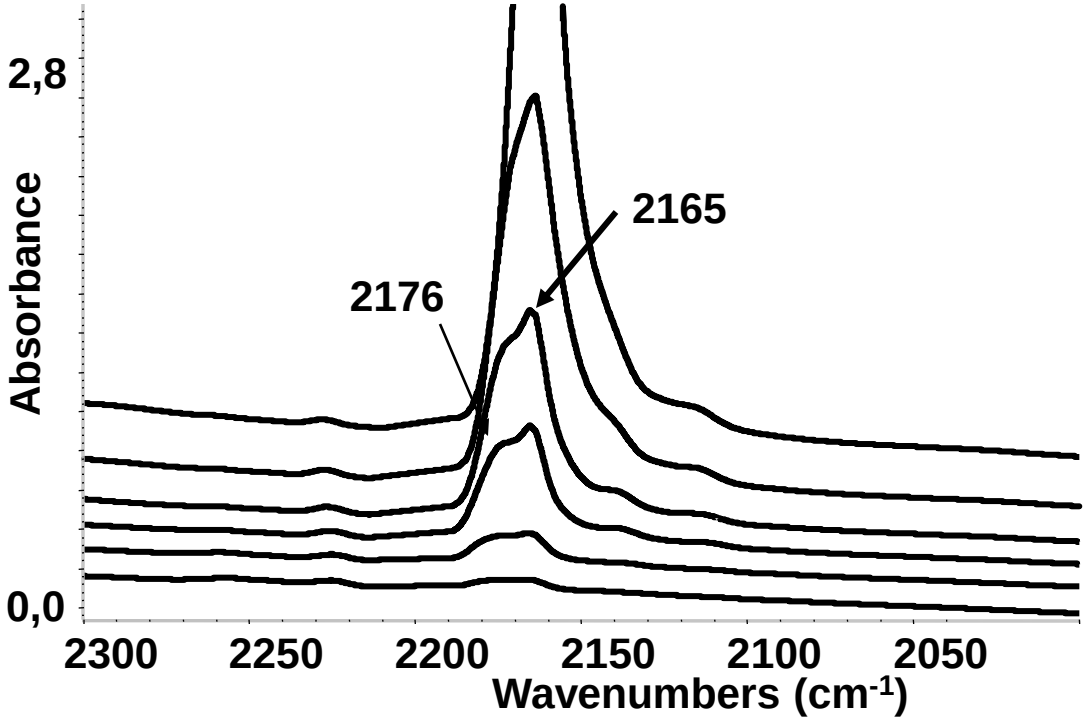
2,8
Absorbance
0,0
2176
2165
2300
2250
2200
2150
2100
2050
Wavenumbers (cm-1)

Figure 5

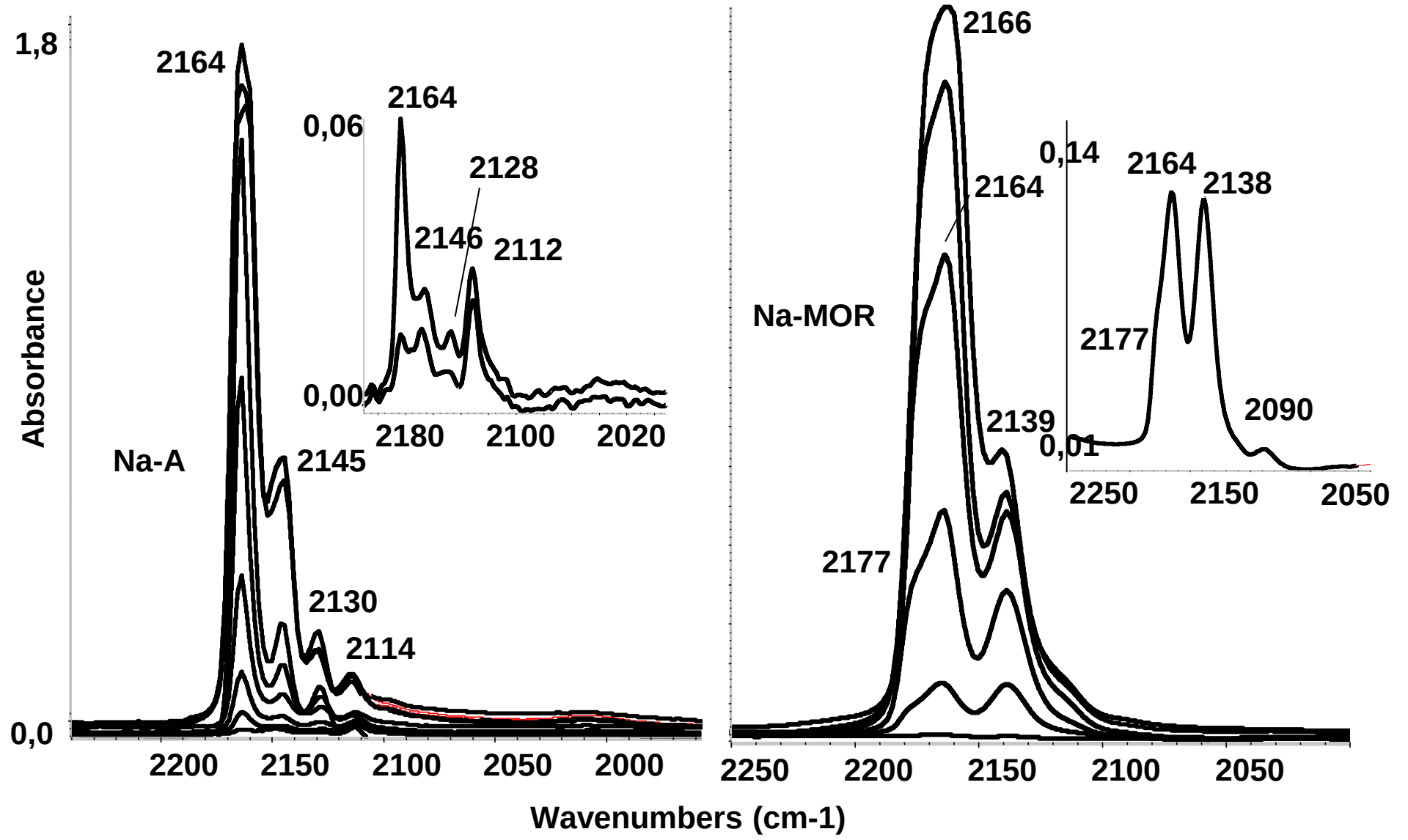
1,8
0,0
Absorbance
Na-A
2164
2145
2130
2114
0,06
0,00
2164
2128
2146
2112
2180
2100
2020
2200
2150
2100
2050
2000
Na-MOR
2166
2164
2177
2139
0,14
0,01
2164
2138
2177
2090
2250
2150
2050
2250
2200
2150
2100
2050
Wavenumbers (cm-1)

Figure 6

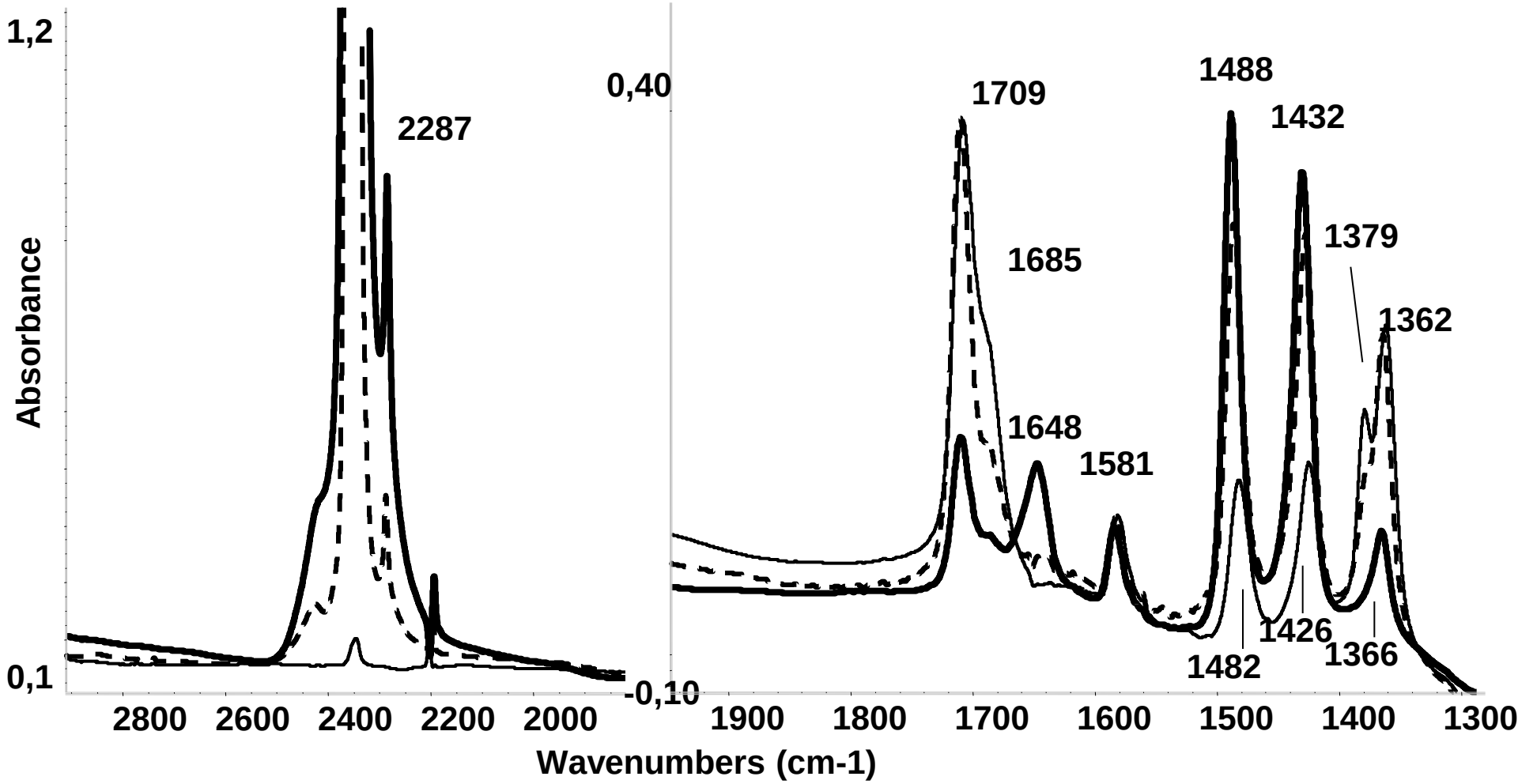
1,2
0,1
Absorbance
2287
0,40
-0,10
1709
1685
1648
1581
1488
1432
1379
1362
1426
1482
1366
2800
2600
2400
2200
2000
1900
1800
1700
1600
1500
1400
1300
Wavenumbers (cm-1)

Figure 7

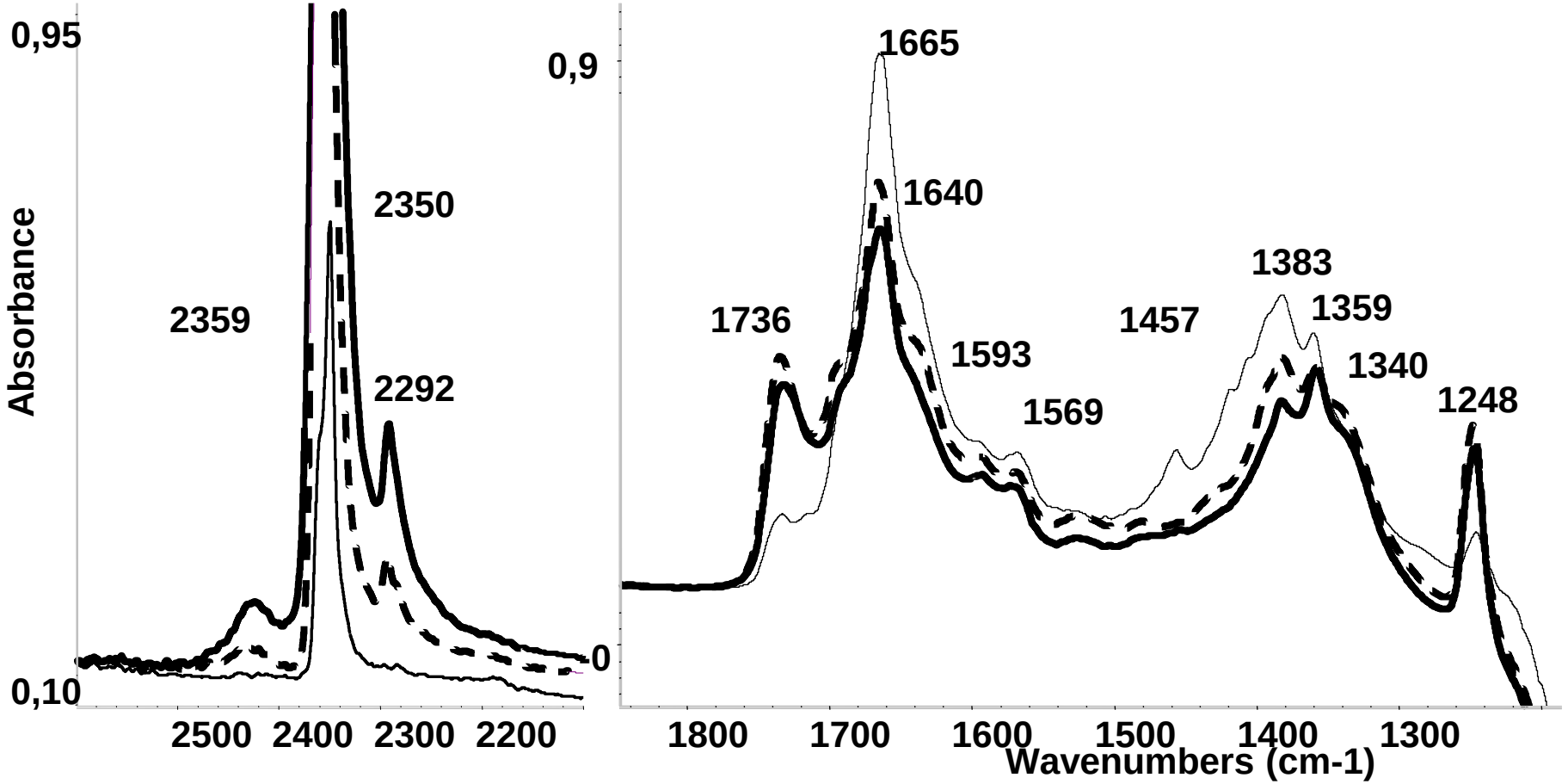
0,95
0,10
Absorbance
2359
2350
2292
2500
2400
2300
2200
0,9
0
1665
1640
1736
1593
1569
1457
1383
1359
1340
1248
1800
1700
1600
1500
1400
1300
Wavenumbers (cm-1)

Figure 8

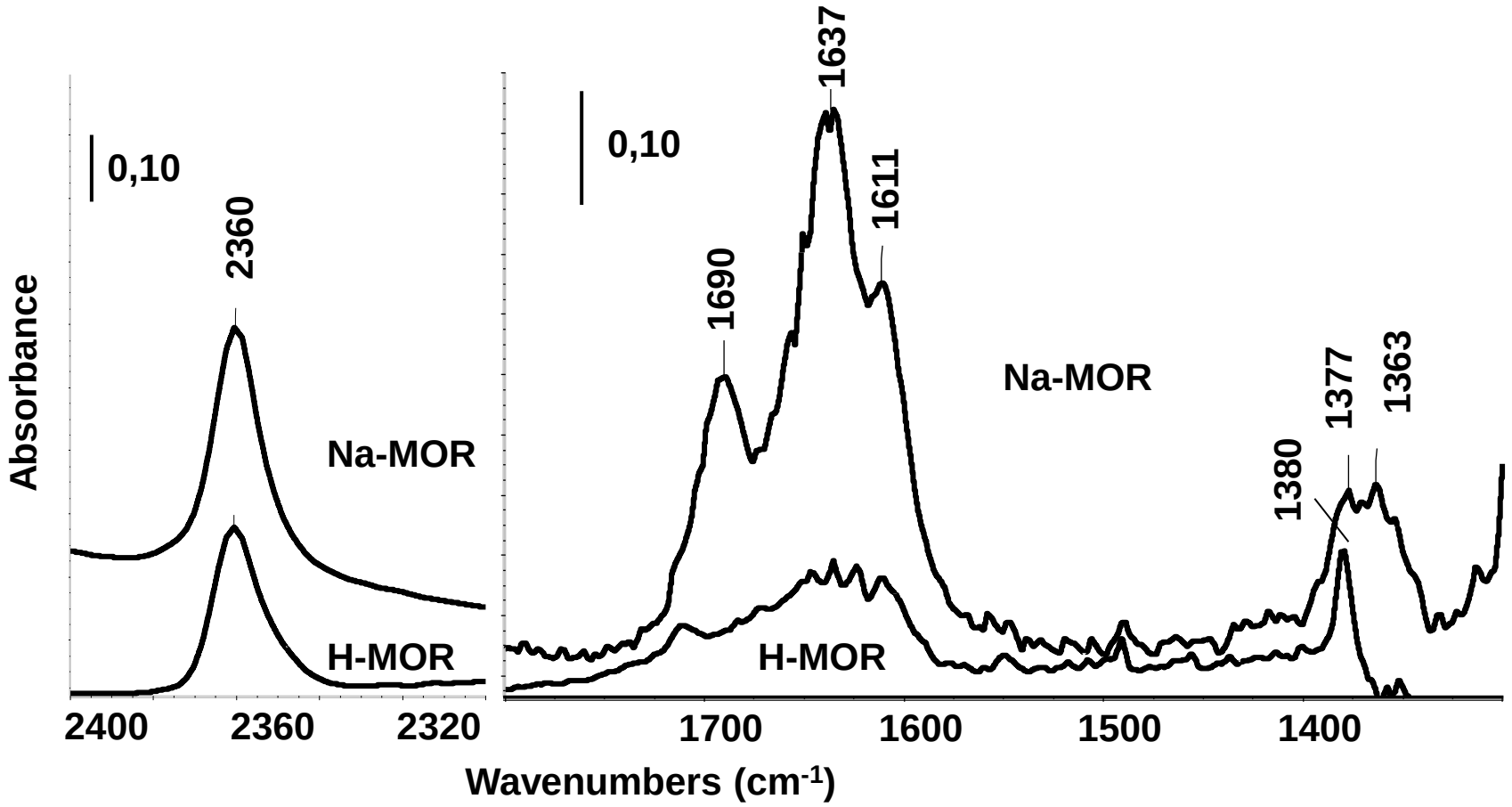
0,10
2360
Na-MOR
H-MOR
Absorbance
2400
2360
2320
0,10
1637
1611
1690
Na-MOR
1380
1377
1363
H-MOR
1700
1600
1500
1400
Wavenumbers (cm-1)

Figure 9

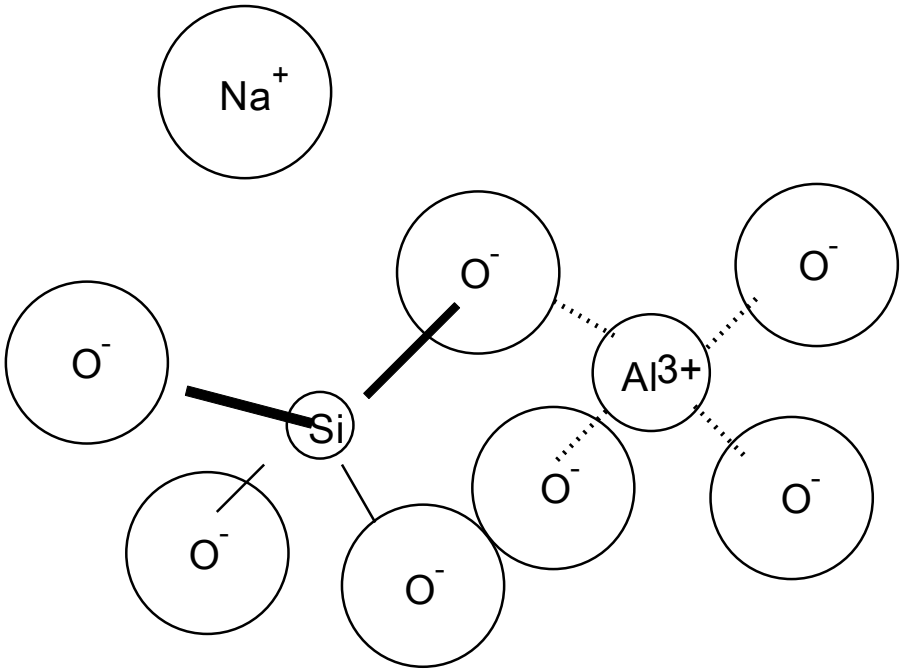

Figure 10

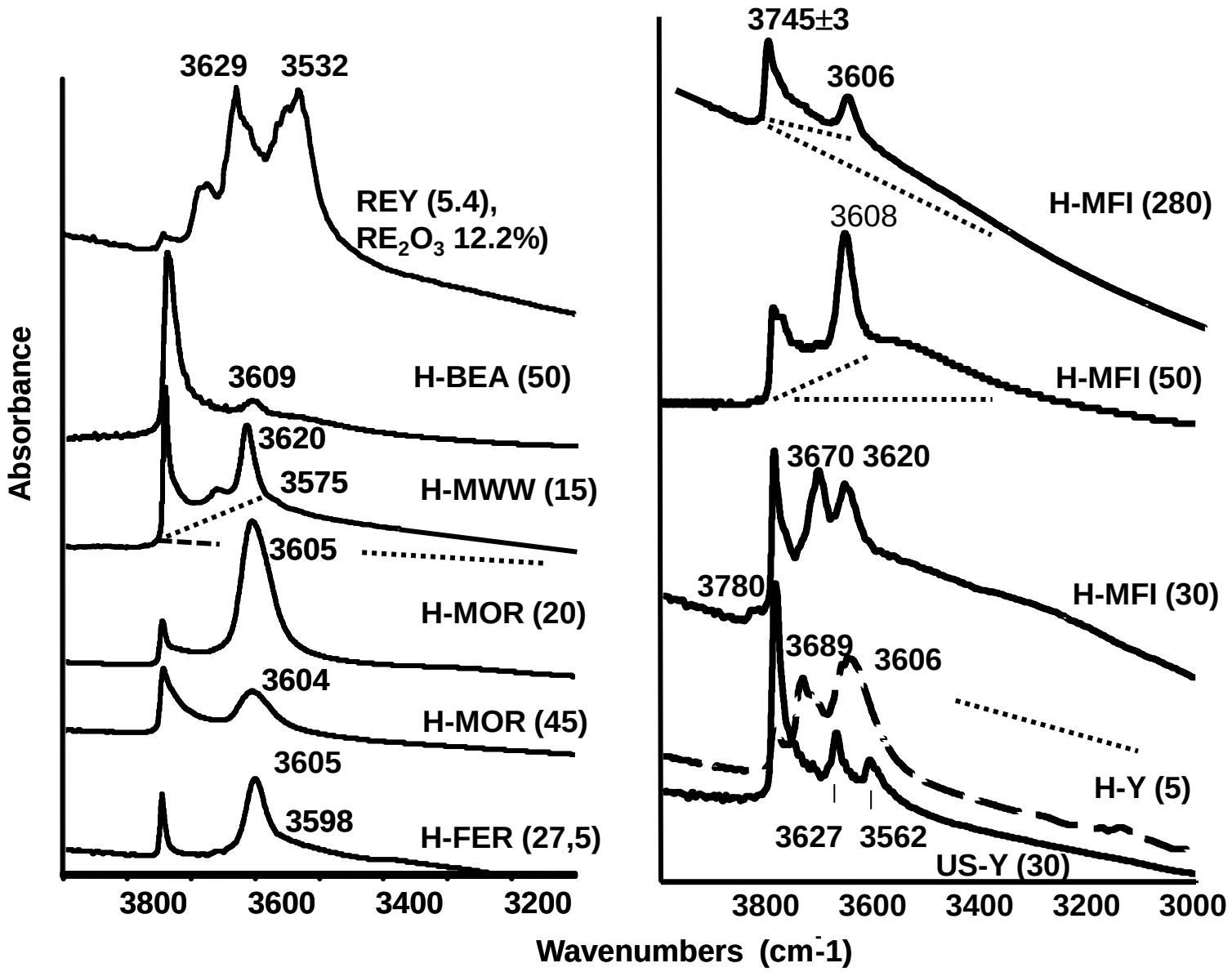
3629
3532
REY (5.4),
RE2O3 12.2%)
3609
H-BEA (50)
3620
3575
H-MWW (15)
3605
H-MOR (20)
3604
H-MOR (45)
3605
3598
H-FER (27,5)
Absorbance
3800
3600
3400
3200
3745±3
3606
H-MFI (280)
3608
H-MFI (50)
3670 3620
3780
H-MFI (30)
3689
3606
H-Y (5)
3627 3562
US-Y (30)
3800
3600
3400
3200
3000
Wavenumbers (cm-1)

Figure 11

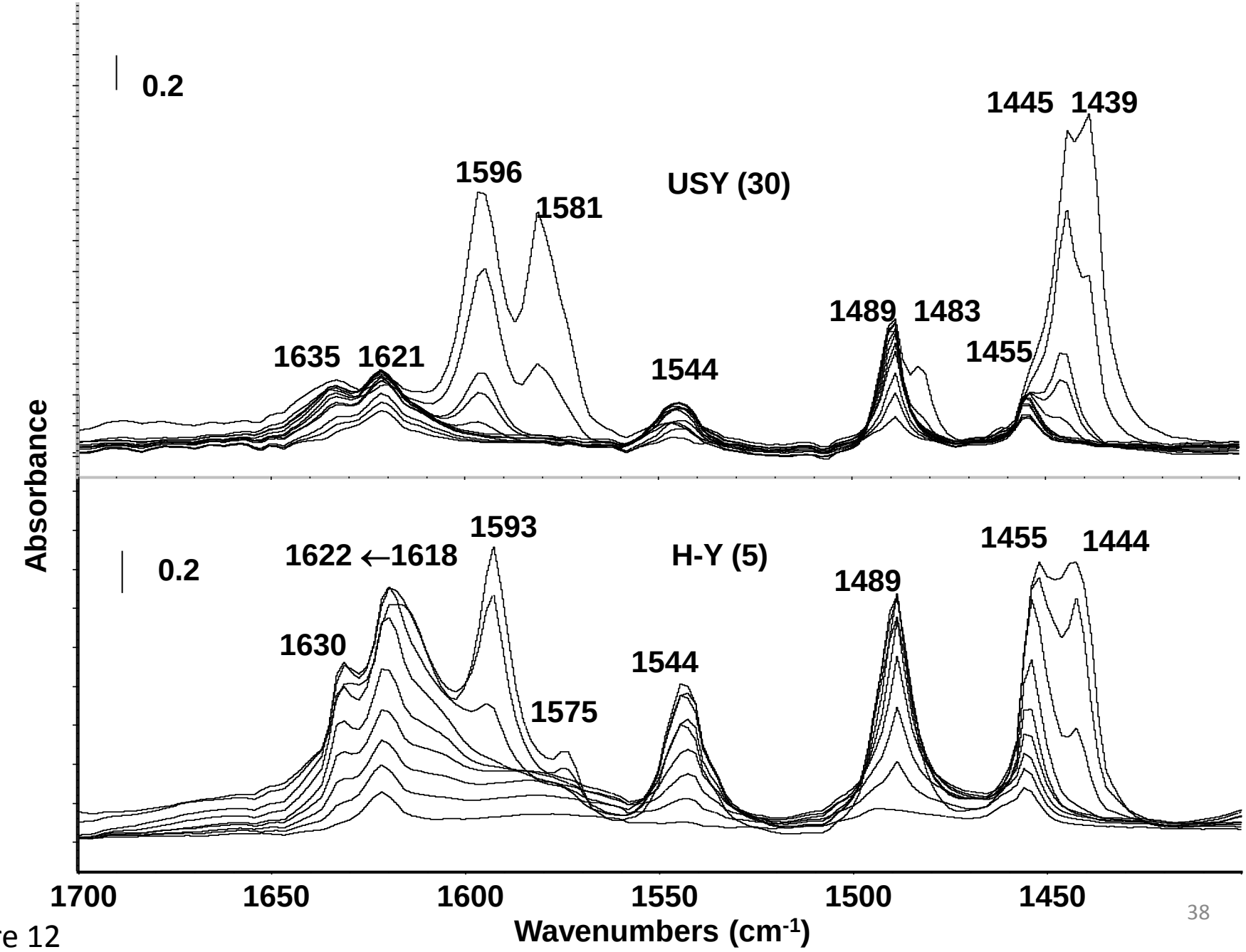
0.2
1445
1439
1596
1581
USY (30)
1489
1483
1635
1621
1455
1544
Absorbance
0.2
1593
1622 ←1618
H-Y (5)
1455
1444
1489
1630
1544
1575
1700
1650
1600
1550
1500
1450
Wavenumbers (cm-1)

Figure 12

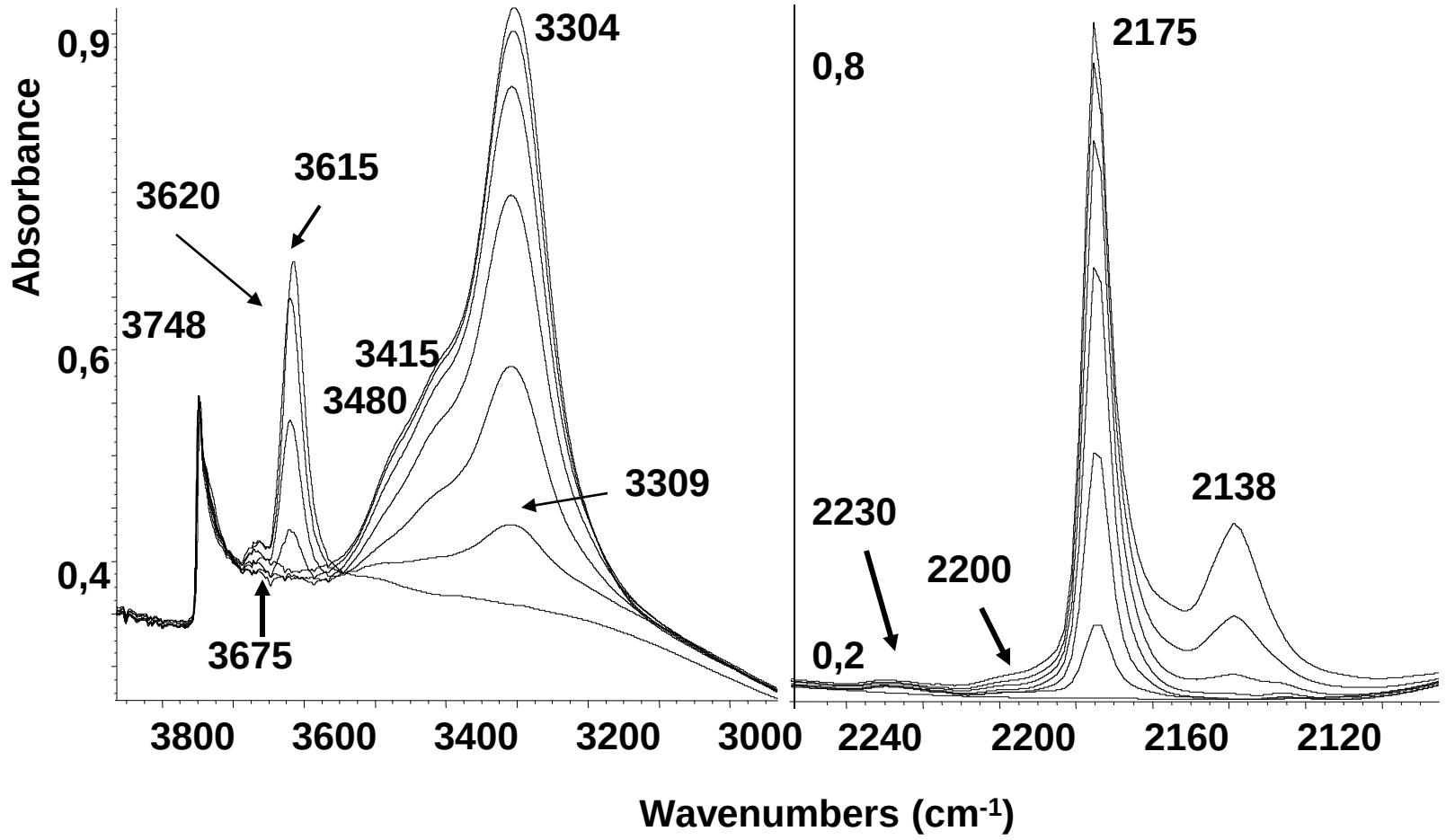
Absorbance
0,9
0,6
0,4
3304
3615
3620
3748
3415
3480
3309
3675
0,8
0,2
2175
2230
2200
2138
3800
3600
3400
3200
3000
2240
2200
2160
2120
Wavenumbers (cm-1)

Fig. 13

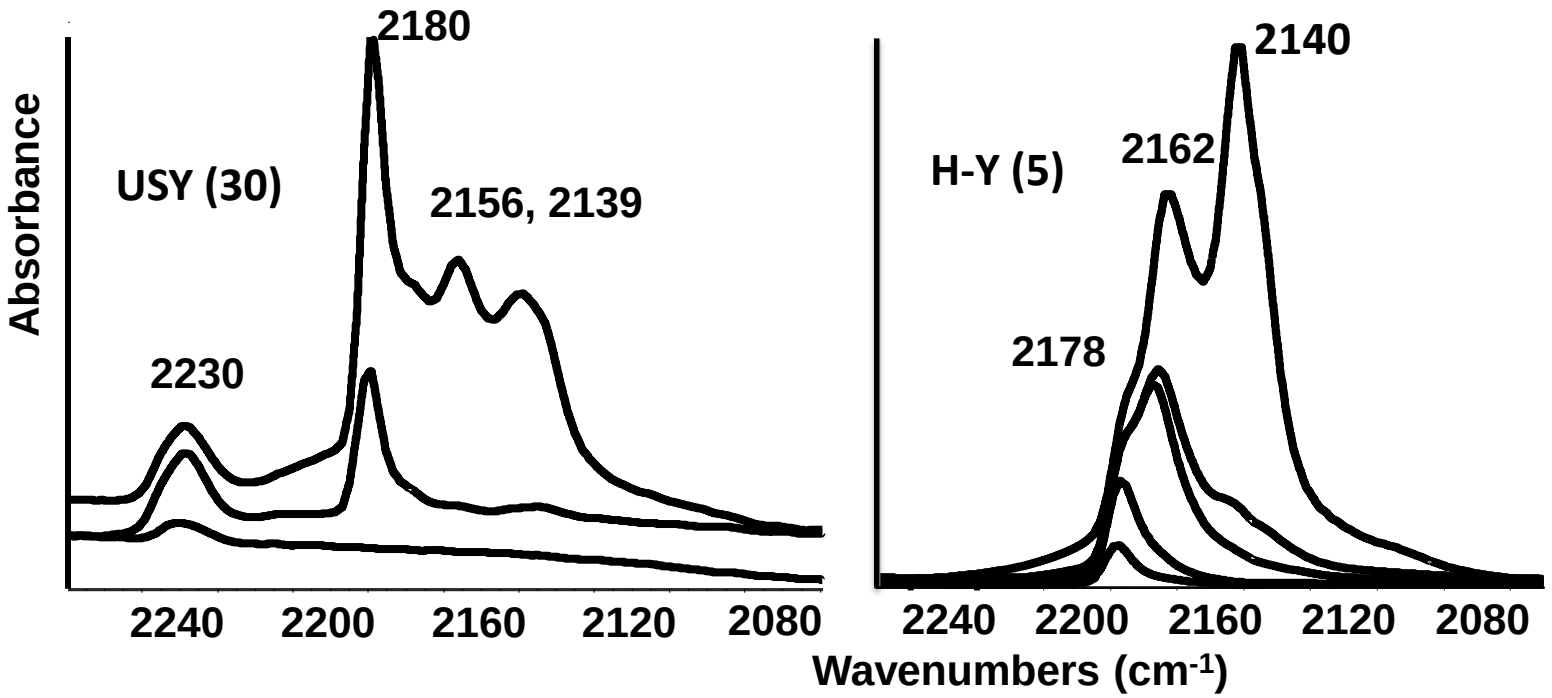
Absorbance
USY (30)
2180
2156, 2139
2230
H-Y (5)
2140
2162
2178
2240 2200 2160 2120 2080
2240 2200 2160 2120 2080
Wavenumbers (cm-1)

Fig. 14

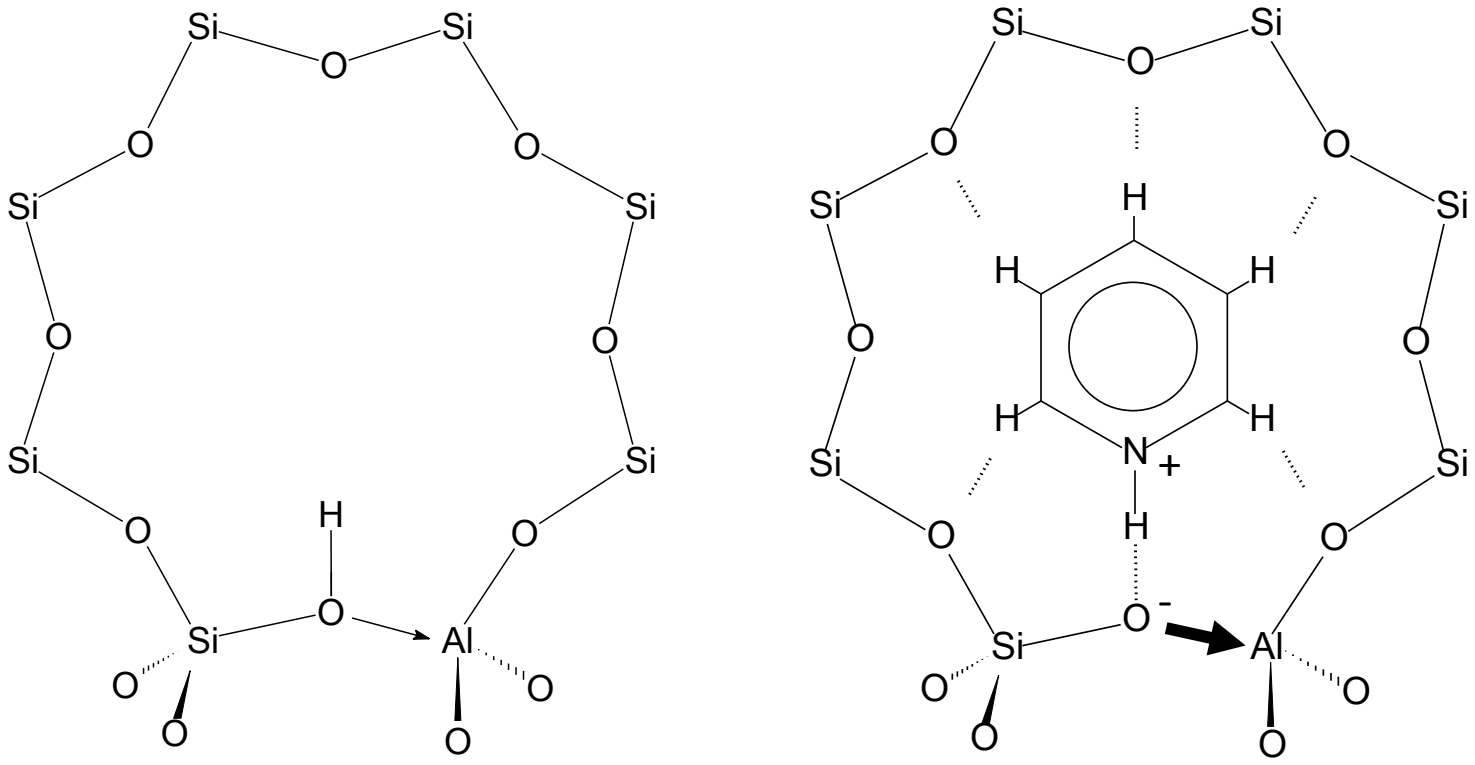
Si
O
Si
O
O
Si
Si
O
O
Si
Si
O
O
Si
H
O
Si
Al
O
O
O
O
O
O
Si
O
Si
O
O
Si
Si
O
O
Si
H
H
H
H
H
H
N
+
H
O
-
Si
Al
O
O
O
O
O
O

Figure 15

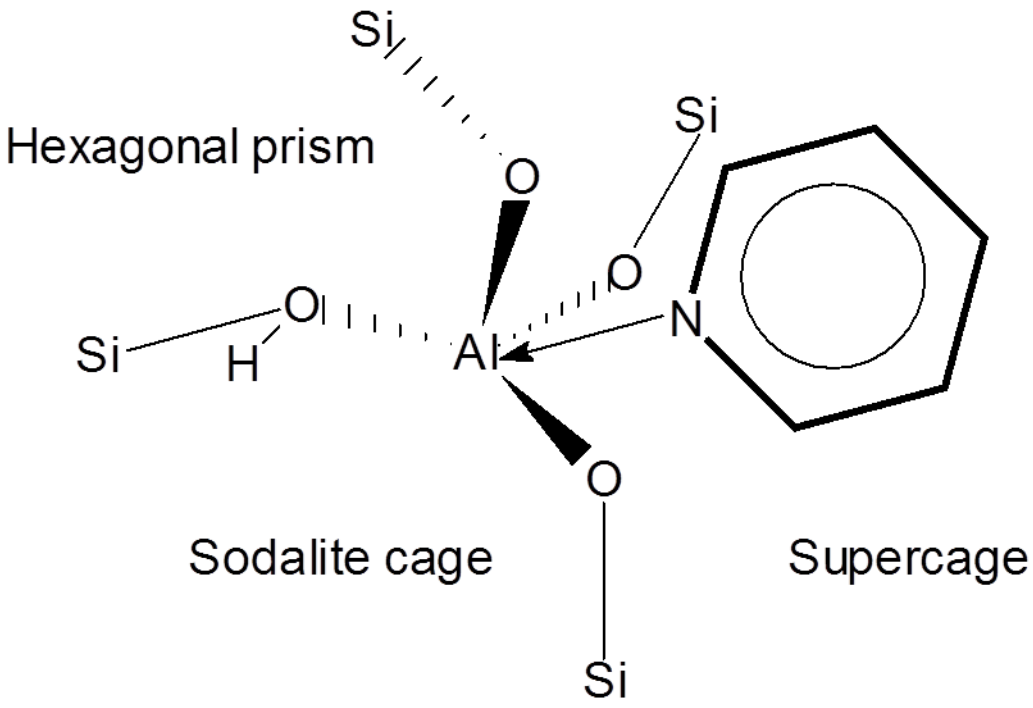
Si
Hexagonal prism
O
Si
O
O
N
Si
H
Al
O
Sodalite cage
Supercage
Si

Fig. 16